NACA

RESEARCH MEMORANDUM

AN INVESTIGATION AT SUBSONIC SPEEDS OF THE ROLLING EFFECTIVENESS OF A SMALL PERFORATED SPOILER ON A WING HAVING 45° OF SWEEPBACK

By Angelo Bandettini

Ames Aeronautical Laboratory
Moffett Field, Calif.

NATIONAL ADVISORY COMMITTEE FOR AERONAUTICS
WASHINGTON
September 15, 1952

NATIONAL ADVISORY COMMITTEE FOR AERONAUTICS

RESEARCH MEMORANDUM

AN INVESTIGATION AT SUBSONIC SPEEDS OF THE ROLLING EFFECTIVENESS OF A SMALL PERFORATED SPOILER ON A WING HAVING 45° OF SWEEPBACK

By Angelo Bandettini

SUMMARY

The rolling effectiveness of a partial-span, perforated spoiler on a wing having 45° of sweepback has been determined at Mach numbers from 0.25 to 0.96. The effects of the spoiler on the lift, drag, and pitching moment were also determined. The spoiler had an average projection of 6.3 percent of the local wing chord and a span of 24.6 percent of the wing semispan. The wing had 45° of sweepback of the leading edge, an aspect ratio of 3, and a taper ratio of 0.4. The thickness-chord ratio parallel to the plane of symmetry was 0.03. The majority of the data were obtained at a test Reynolds number of 1,500,000; however, at a Mach number of 0.25 the Reynolds number was varied from 1,500,000 to 6,000,000.

The spoiler was effective in producing a rolling moment of the proper sign at angles of attack less than about 12° at all Mach numbers and Reynolds numbers of the test. The magnitude of rolling-moment coefficient increased with increasing angle of attack up to an angle of attack between 2° and 4° and then generally decreased with further increase in angle of attack. At the higher angles of attack the effectiveness of the spoiler was small and control reversal was encountered for some test conditions.

The rate of roll resulting from projection of the spoiler has been estimated, using calculated values of damping in roll and the rolling-moment coefficients obtained from the tests. The predicted helix angle generated by the wing tip in a steady roll increased with increasing Mach number up to a Mach number of 0.90 and then was relatively constant as the Mach number was further increased to 0.94.

INTRODUCTION

Lateral control by means of spoilers offers certain advantages over conventional ailerons for high-speed aircraft with thin swept-back wings. The low torsional rigidity of such wings results in large amounts of wing twist when ailerons near the wing tips are deflected at high flight speeds, with a resultant deterioration of the rolling power afforded by the ailerons. Because of the smaller twisting moment resulting from spoiler projection, these aeroelastic effects are not so pronounced when a spoiler is used as a lateral control.

Even when aeroelastic effects are small, the rolling effectiveness of flap-type ailerons deteriorates more severely at transonic speeds than that of spoilers. Also the more favorable yawing characteristics of the spoilers become increasingly important for highly swept wings with their high dihedral effect.

When spoilers alone are used as the lateral control, the attainment of adequate rolling effectiveness at low speeds is sometimes difficult. Also the drag of a large spoiler, while it does produce favorable yawing moments, may be of sufficient magnitude to cause abrupt changes in speed during rolling maneuvers.

To overcome some of these difficulties and still take advantage of the effectiveness of spoilers at high speeds, the use of small spoilers in combination with conventional ailerons appears attractive for certain types of high-performance airplanes. The lateral control characteristics of such a wing-spoiler-aileron combination have been determined by rocket-model tests at 0° angle of attack and reported in reference 1. The purpose of the present investigation was to obtain lateral control data throughout the subsonic speed range on a similar wing-spoiler combination over a range of angles of attack.

NOTATION

b wing span

c local wing chord, measured parallel to plane of symmetry

$\bar{c}$ wing mean aerodynamic chord $\left(\dfrac{\int_0^{b/2} c^2 dy}{\int_0^{b/2} c\, dy}\right)$

C_D drag coefficient $\left(\dfrac{\text{drag}}{qS}\right)$

C_L lift coefficient $\left(\frac{\text{lift}}{qS}\right)$

C_l rolling-moment coefficient due to spoiler taken about the body axis

$$\left(\frac{\text{rolling moment with spoiler - rolling moment without spoiler}}{qSb}\right)$$

C_{l_p} damping in roll, rate of change of rolling-moment coefficient, C_l, with wing-tip helix angle $\left(\frac{pb}{2V}\right)$, per radian

C_m pitching-moment coefficient about the 25-percent point of the wing mean aerodynamic chord $\left(\frac{\text{pitching moment}}{qS\bar{c}}\right)$

l length of body including portion removed to accommodate sting

M Mach number

p rolling angular velocity, radians per second

$\frac{pb}{2V}$ helix angle generated by the wing tip in a steady roll, radians

q free-stream dynamic pressure

R Reynolds number based on mean aerodynamic chord

r radius of body

r_o maximum body radius

S total wing area, including area formed by extending the leading and trailing edges to the plane of symmetry

t maximum thickness of wing section

V free-stream velocity

x longitudinal distance from nose of body

x' distance along chord

y distance perpendicular to plane of symmetry

z distance perpendicular to chord of wing

α angle of attack of the body axis, degrees

ΔC_L incremental lift coefficient due to spoiler

ΔC_D incremental drag coefficient due to spoiler

ΔC_m incremental pitching-moment coefficient due to spoiler

WIND-TUNNEL AND TEST VARIABLES

The experimental investigation was conducted in the Ames 12-foot pressure wind tunnel. Lift, drag, pitching-moment, and rolling-moment data for the model with and without the spoiler were obtained over a Mach number range of 0.25 to 0.96 at a Reynolds number of 1,500,000. Data were also obtained at Reynolds numbers of 3,000,000 and 6,000,000 at a Mach number of 0.25. The angle-of-attack range was varied from -0.7° to $+26^{\circ}$. At the higher Mach numbers and Reynolds numbers vibration of the model, model strength, or wind-tunnel power limited the maximum angles of attack to less than 26°. All tests were made at an angle of sideslip of 0°.

MODEL

A photograph of the model mounted on the sting support of the Ames 12-foot pressure wind tunnel is shown in figure 1(a). Photographs of the spoiler are shown in figure 1(b). A drawing of the model showing spoiler location is given in figure 2(a) and figure 2(b) is a sketch of the spoiler showing pertinent dimensions.

The wing had a leading-edge sweep of 45°, an aspect ratio of 3, and a taper ratio of 0.4. The airfoil sections parallel to the plane of symmetry were 3-percent-thick biconvex sections described by the equation

$$\frac{z}{c} = 2\left(\frac{t}{c}\right)\left(\frac{x'}{c}\right)\left(1-\frac{x'}{c}\right)$$

No dihedral or incidence was employed and the root chord coincided with the longitudinal center line of the fuselage. The fuselage was a body of revolution described by the equation shown in figure 2. The wings of the model were constructed of solid steel. The model without the spoiler was the same as that used in the tests reported in references 2 and 3, except that for the present tests 5.68 inches were removed from the afterportion of the body.

The average projection of the spoiler was 6.3 percent of the local wing chord and the length was 24.6 percent of the semispan. The spoiler was mounted on the upper surface of the left wing along the 69-percent-chord line and centered at 54 percent of the semispan. The perforations and the gap between the lower surface of the spoiler and the wing surface accounted for 34.3 percent of the spoiler area. The spoiler was constructed of brass sheet and held in position from the rear by two triangular brackets mounted parallel to the body center line. Design and location of the spoiler was similar to that of the spoiler investigated in reference 1.

The model was mounted on a sting which had a diameter equal to 92 percent of the body base diameter. A balance mounted on the sting and enclosed within the body of the model was used to measure aerodynamic forces and moments on the model. The balance was the 4-inch-diameter, four-component, strain-gage balance illustrated in reference 4.

CORRECTIONS

The test data have been reduced to standard NACA coefficient form. The corrections applied are discussed in the following paragraphs.

Tunnel-Wall Interference

Corrections to the results for the induced effects of the tunnel walls, resulting from lift on the model, were made according to the method of reference 5. The numerical values of these corrections (which were added to the uncorrected data) were the same as in reference 3. No corrections were made to the pitching-moment or rolling-moment coefficients.

The effects of constriction of the flow by the tunnel walls were taken into account by the method of reference 6. This correction was calculated for conditions of 0° angle of attack and was applied throughout the angle-of-attack range. The magnitudes of the correction applied to the Mach number and to the dynamic pressure are shown in the following table:

Corrected Mach number	Uncorrected Mach number	$\frac{q_{corrected}}{q_{uncorrected}}$
0.250	0.250	1.001
.600	.600	1.001
.800	.799	1.002
.850	.848	1.003
.900	.896	1.004
.920	.916	1.005
.940	.934	1.007
.960	.950	1.010

Stream Variations

Calibration of the 12-foot wind tunnel has shown that in the test region the stream inclination determined from tests of a wing spanning the tunnel, with the support system at 0° angle of attack, is less than 0.08°. The longitudinal variation of static pressure in the region of the model is less than 0.9 percent of the dynamic pressure in this region. No correction for the effect of these stream variations was made.

Support Interference

The effects of support interference on the aerodynamic characteristics of the model are not known. For the present tailless model, it is believed that such effects consisted primarily of a change in the pressure at the base of the model. In an effort to correct at least partially for this support interference, the base pressure was measured and the drag data were adjusted to correspond to a base pressure equal to the static pressure of the free stream.

Aeroelastic Effects

No corrections for wing bending or twisting have been applied. It is assumed such corrections were negligible for the steel wing operating at the test conditions of this investigation.

RESULTS AND DISCUSSION

Reynolds Number

The effects of increasing the Reynolds number from 1,500,000 to 6,000,000 on the characteristics of the model at a Mach number of 0.25 are shown in figure 3. At all Reynolds numbers of the test, the spoiler was effective in producing a rolling moment of the proper sign at angles of attack less than 16°. Figure 3(a) shows that the angle of attack at which the rolling moment reached a maximum was between 2° and 4° with a rapid decrease in effectiveness as the angle of attack was further increased. For angles of attack between 4° and 16° there was an increase in rolling-moment coefficient with increasing Reynolds number. Reynolds number variation had little effect on the small incremental lift, drag, and pitching-moment coefficients due to the spoiler (figs. 3(a) and 3(b)).

Mach Number

The variations of rolling-moment coefficient with angle of attack at Mach numbers from 0.25 to 0.96 and a Reynolds number of 1,500,000 are presented in figures 3 to 10. At all Mach numbers of the test, the spoiler was effective in producing a rolling moment of the proper sign at angles of attack less than about 12°. The magnitude of the rolling-moment coefficient increased with increasing angle of attack above 0° and reached a maximum value at an angle of attack between 2° and 4°. At the higher angles of attack the rolling-moment coefficients became small and control reversal occurred at several Mach numbers. At Mach numbers below 0.85, a slight increase in the magnitude of the rolling-moment coefficient with increasing angle of attack was evident near 8° angle of attack. Figure 11 shows that the rolling-moment coefficient generally increased with increasing Mach number up to a Mach number of 0.94 for angles of attack up to 8°.

Addition of the perforated spoiler to the plain wing resulted in a reduction in lift coefficient at low angles of attack and very little change in lift coefficient at high angles of attack (figs. 3(a) to 10(a)). At small angles of attack, increasing the Mach number from 0.25 to 0.85 caused an algebraic decrease in the incremental lift coefficient due to the spoiler, but a further increase in Mach number to 0.96 had little effect (fig. 12). The incremental drag coefficient resulting from projection of the spoiler was approximately 0.0060 at small angles of attack and low Mach numbers and in general increased with increasing Mach number (fig. 13). In figures 3(b) through 10(b) it is shown that projection of the perforated spoiler at low angles of attack resulted in a forward movement of the wing center of pressure. Figure 14 shows an increase with increasing Mach number of the incremental pitching-moment coefficient due to the spoiler.

Predicted Rate of Roll

In order to evaluate the performance of the spoiler in terms of the usual criteria for lateral controls, the rate of roll due to spoiler projection has been calculated using the damping in roll determined by the method of reference 7. Results of calculations which account for the effects of sweep, taper ratio, aspect ratio, and Mach number are shown in figure 15. The rolling performance, as defined by the helix angle generated by the wing tip in a steady roll $pb/2V$, is presented in figure 16 as a function of Mach number. These calculations are based on the rolling moment produced by the spoiler at an angle of attack of 0°. Correction was made for the induced angle of attack at the spoiler location due to the rolling velocity. Comparison on the basis of a complete wing with only one spoiler is made between the values of $pb/2V$ predicted from the measured rolling moment and the values of $pb/2V$ obtained during a rocket-model investigation of a similar wing-spoiler combination (reference 1.) The agreement is good.

The values of $pb/2V$ obtained in the present tests increased with increasing Mach number from a value of 0.020 at a Mach number of 0.25 to a value of 0.038 at a Mach number of 0.90, but changed little with an increase in Mach number to 0.94. Further increase in Mach number to 0.96 resulted in a decrease in $pb/2V$ to a value of 0.033. The theoretical values of the damping in roll become increasingly unreliable as the Mach number approaches 1.0 and the decrease in $pb/2V$ at the highest Mach number may result from too high an estimated value of C_{l_p}. It is also possible that this decrease in rate of roll at the highest Mach number is a result of tunnel-wall interference. However, the rocket-model investigation of reference 1 also indicated a decrease in $pb/2V$ as the Mach number was increased at high subsonic speeds (fig. 16).

The predicted rate of roll at Mach numbers near unity is approximately 42 percent of the rate of roll specified in reference 8 for fighter-type aircraft. As noted in a previous section of the report, the spoiler investigated is of a type and size which would be expected to augment the lateral control provided by conventional ailerons rather than to provide the entire lateral control for the aircraft. Reference 1 shows that an aileron of moderate chord, extending from the outer edge of the spoiler to the wing tip, in conjunction with the spoiler, provided effective control even in the presence of severe aeroelastic effects.

CONCLUDING REMARKS

The results of an investigation throughout the subsonic Mach number range to determine the rolling effectiveness and other aerodynamic characteristics resulting from projection of a perforated spoiler on a wing having a sweepback of 45° and aspect ratio of 3 have been presented.

The spoiler was effective in producing a rolling moment of the proper sign at angles of attack less than 12° at all Mach numbers. At angles of attack less than 10° the rolling-moment coefficient increased with increasing Mach number up to a Mach number of 0.94. The value of the rolling-moment coefficient reached a maximum at an angle of attack between 2° and 4° and then generally decreased with further increase of angle of attack. At the higher angles of attack the control effectiveness was very small and for some test conditions a control reversal was evident. The incremental drag coefficient resulting from projection of the spoiler was approximately 0.0060 at small angles of attack and low Mach numbers and, in general, increased with Mach number. The predicted values of the helix angle generated by the wing tip in a steady roll at an angle of attack of 0° (using values of C_{l_p} computed from theory) increased with increasing Mach number up to a Mach number of 0.90 and varied little with a further increase in Mach number to 0.94.

Ames Aeronautical Laboratory
National Advisory Committee for Aeronautics
Moffett Field, California

REFERENCES

1. Strass, H. Kurt, and Marley, Edward T.: Rocket-Model Investigation of the Rolling Effectiveness of a Fighter-Type Wing-Control Configuration at Mach Numbers from 0.6 to 1.5. NACA RM L51I28, 1952.

2. Heitmeyer, John C.: Lift, Drag, and Pitching Moment of Low-Aspect-Ratio Wings at Subsonic and Supersonic Speeds - Plane 45° Swept-Back Wing of Aspect Ratio 3, Taper Ratio 0.4 With 3-Percent-Thick, Biconvex Section. NACA RM A51H10, 1951.

3. Smith, Donald W., Shibata, Harry H., and Selan, Ralph: Lift, Drag, and Pitching Moment of Low-Aspect-Ratio Wings at Subsonic and Supersonic Speeds - An Investigation at Large Reynolds Numbers of the Low-Speed Characteristics of Several Wing-Body Combinations. NACA RM A51K28, 1952.

4. Olson, Robert N., and Mead, Merrill H.: Aerodynamic Study of a Wing-Fuselage Combination Employing a Wing Swept Back 63° - Effectiveness of an Elevon on a Longitudinal Control and the Effects of Camber and Twist on the Maximum Lift-Drag Ratio at Supersonic Speeds. NACA RM A50A31a, 1950.

5. Glauert, H.: Wind Tunnel Interference on Wings, Bodies, and Airscrews. R. & M. No. 1566, British, 1933.

6. Herriot, John G.: Blockage Corrections for Three-Dimensional-Flow Closed-Throat Wind Tunnels, with Consideration of the Effect of Compressibility. NACA Rep. 995, 1950. (Formerly NACA RM A7B28)

7. Bird, John D.: Some Theoretical Low-Speed Span Loading Characteristics of Swept Wings in Roll and Sideslip. NACA Rep. 969, 1950. (Formerly NACA TN 1839)

8. Anon: Specification of Flying Qualities of Piloted Airplanes. BuAer Specifications, NAVAER SR-119B, 1948.

(a) Model.

Figure 1.– Model with spoiler mounted in the Ames 12–foot pressure wind tunnel.

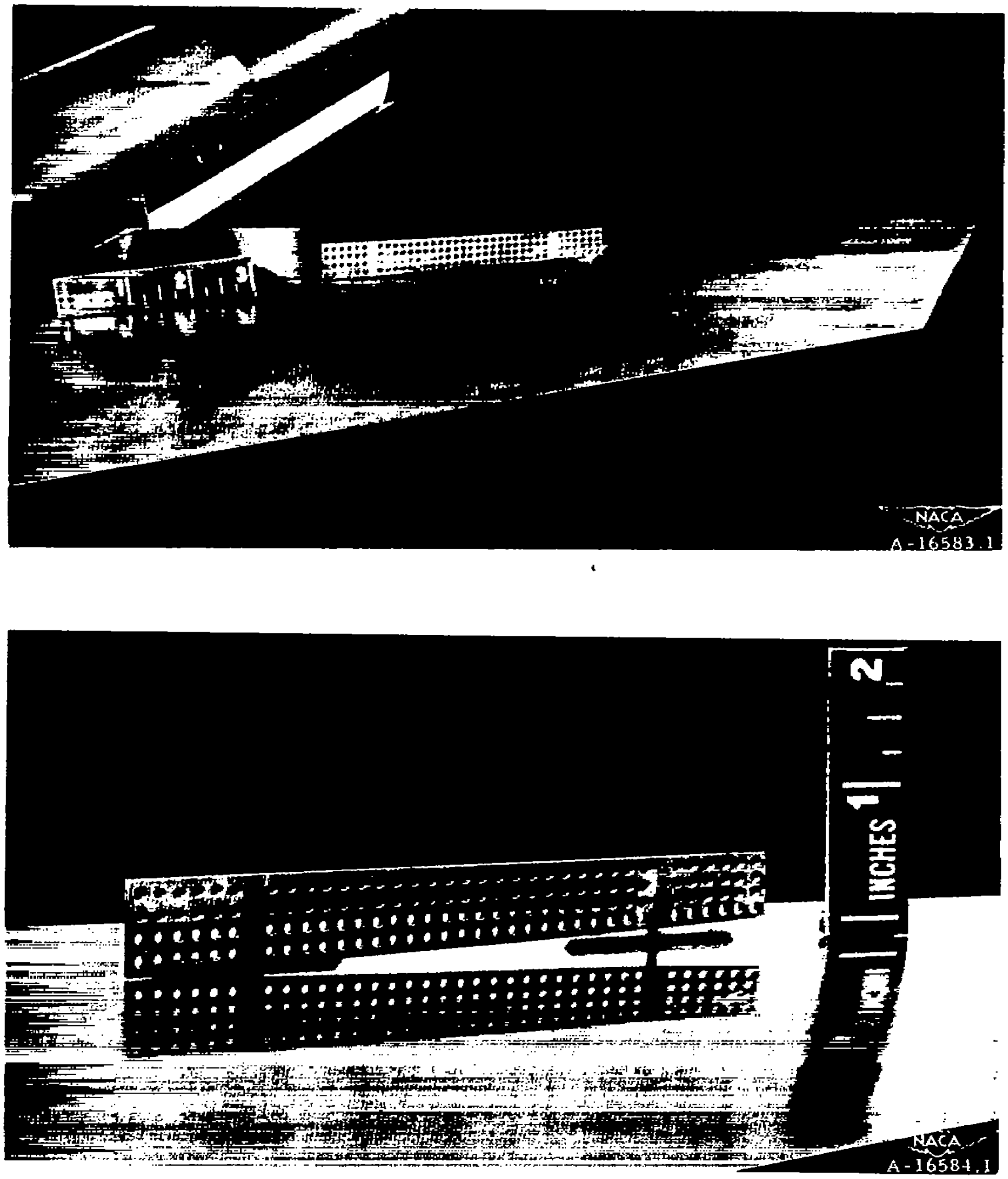

(b) Front and close-up views of spoiler.

Figure 1.– Concluded.

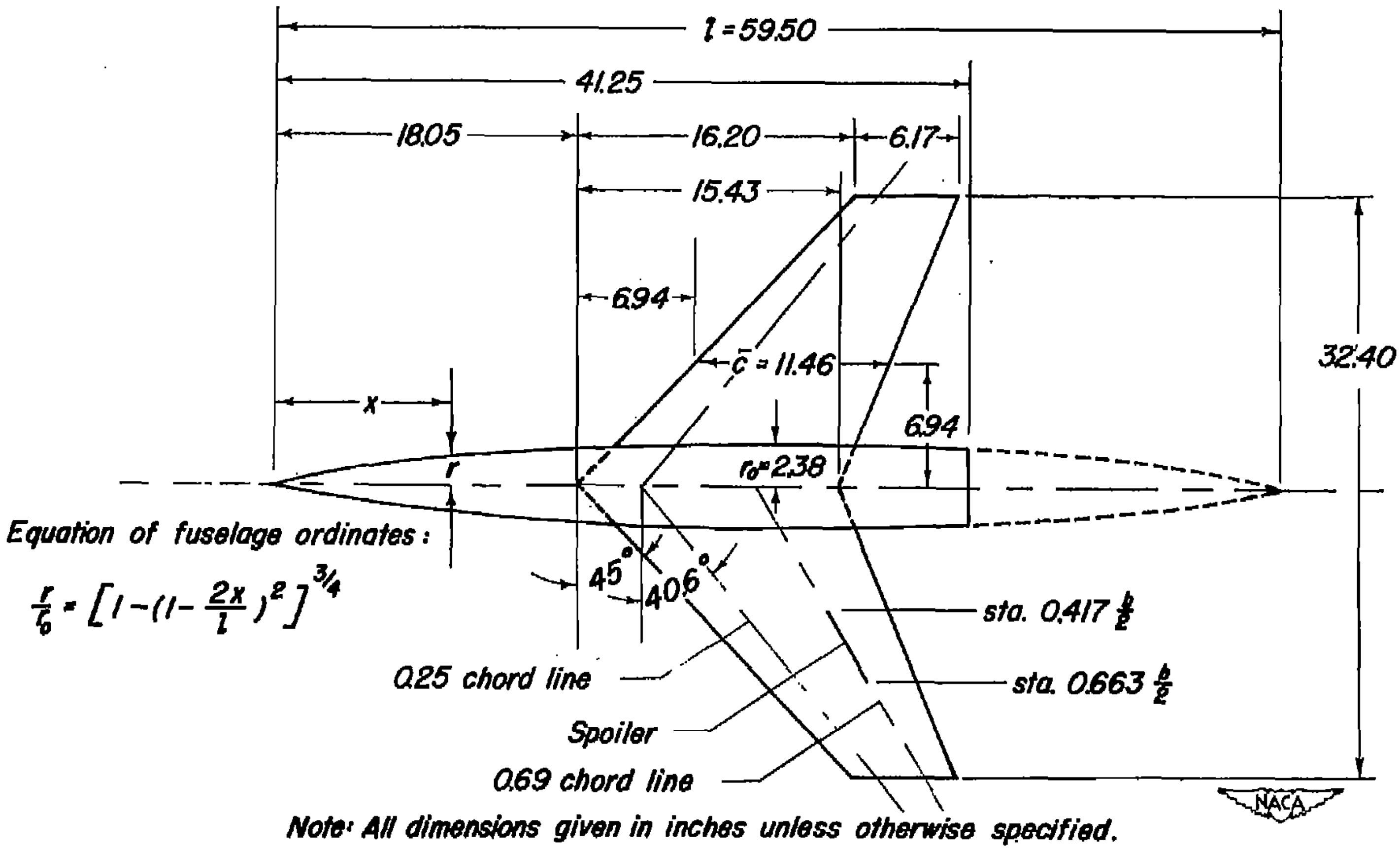

(a) Full-span model showing spoiler location.

Figure 2.– Sketches of model and spoiler.

[redacted]

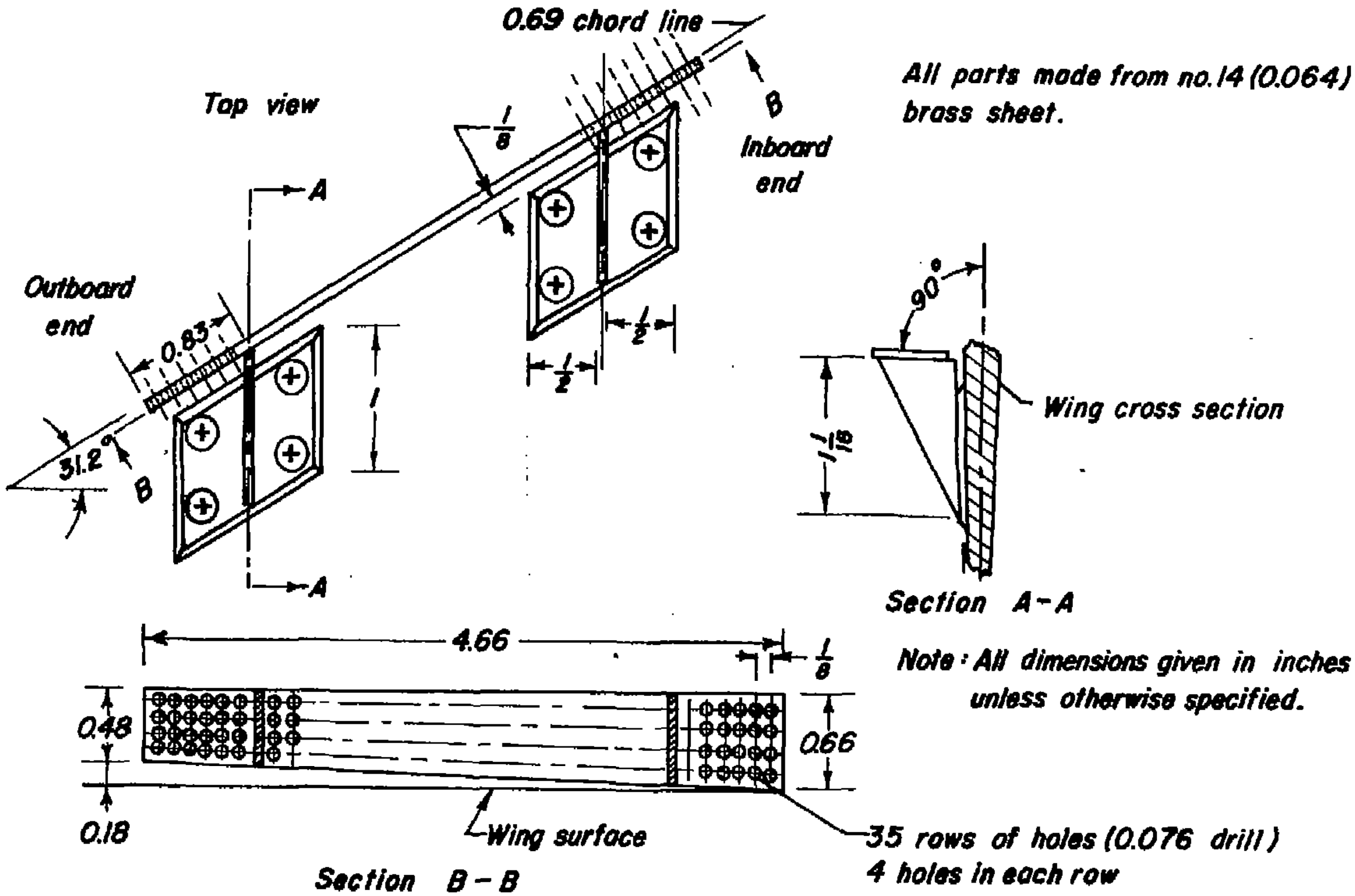

(b) Spoiler details.

Figure 2.- Concluded.

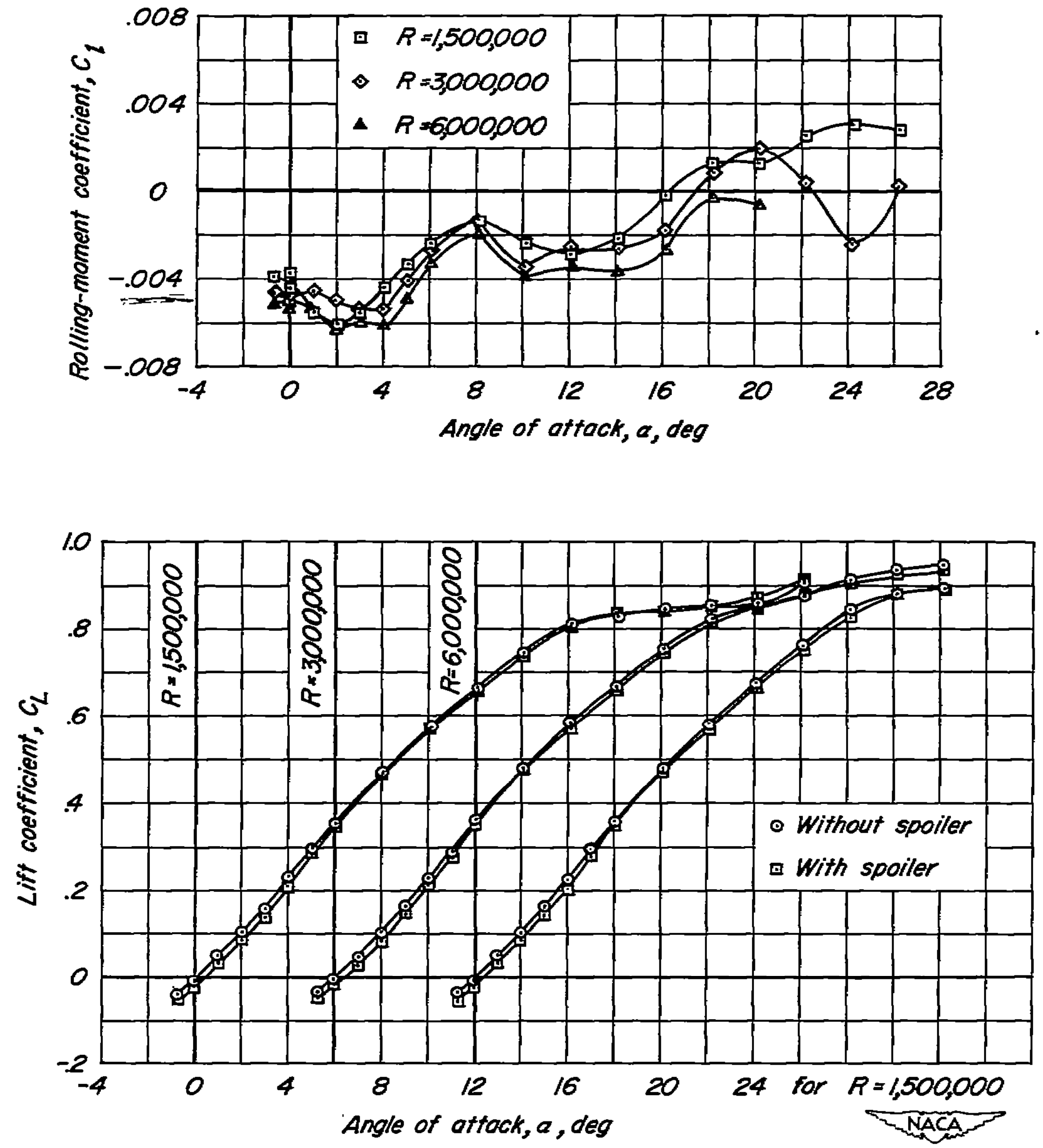

(a) C_l vs α, C_L vs α

Figure 3.– The aerodynamic characteristics at Reynolds numbers of 1,500,000, 3,000,000, and 6,000,000. M = 0.25.

[redacted]

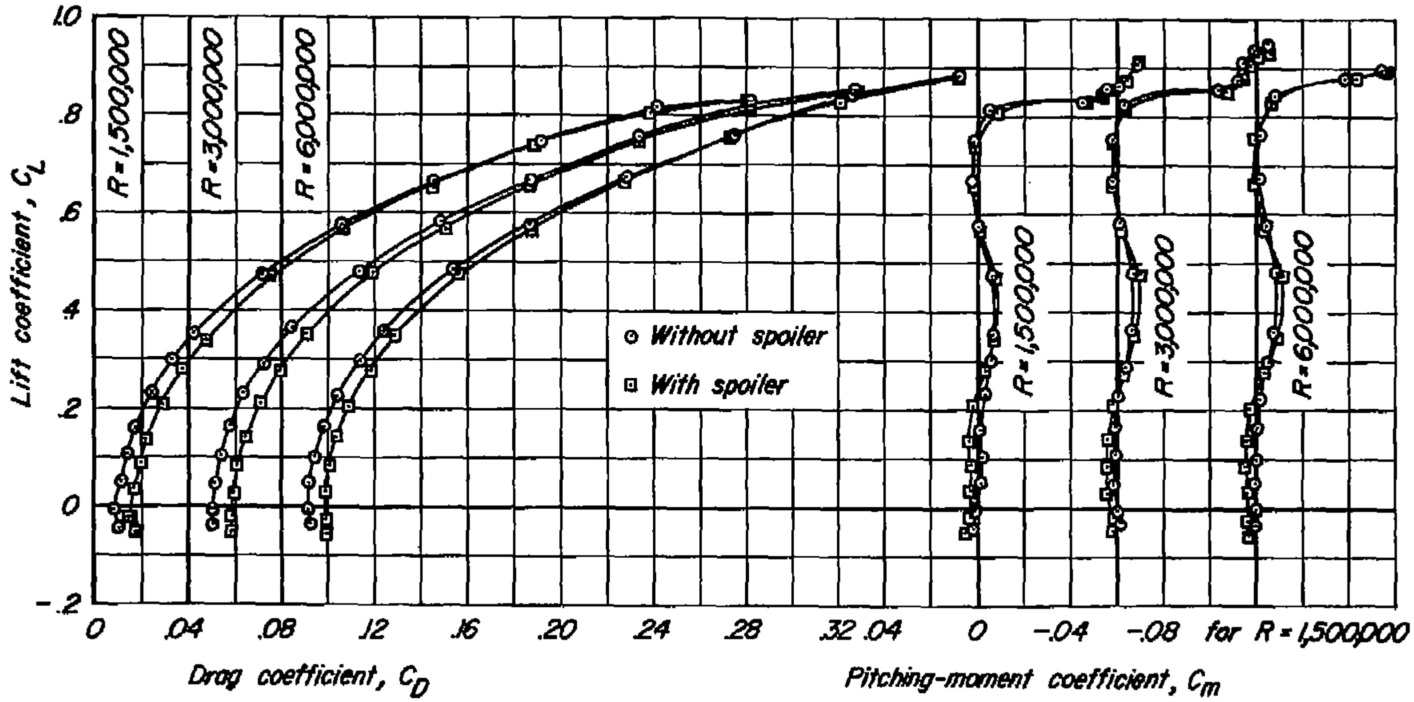

(b) C_L vs C_D, C_L vs C_m

Figure 3.- Concluded.

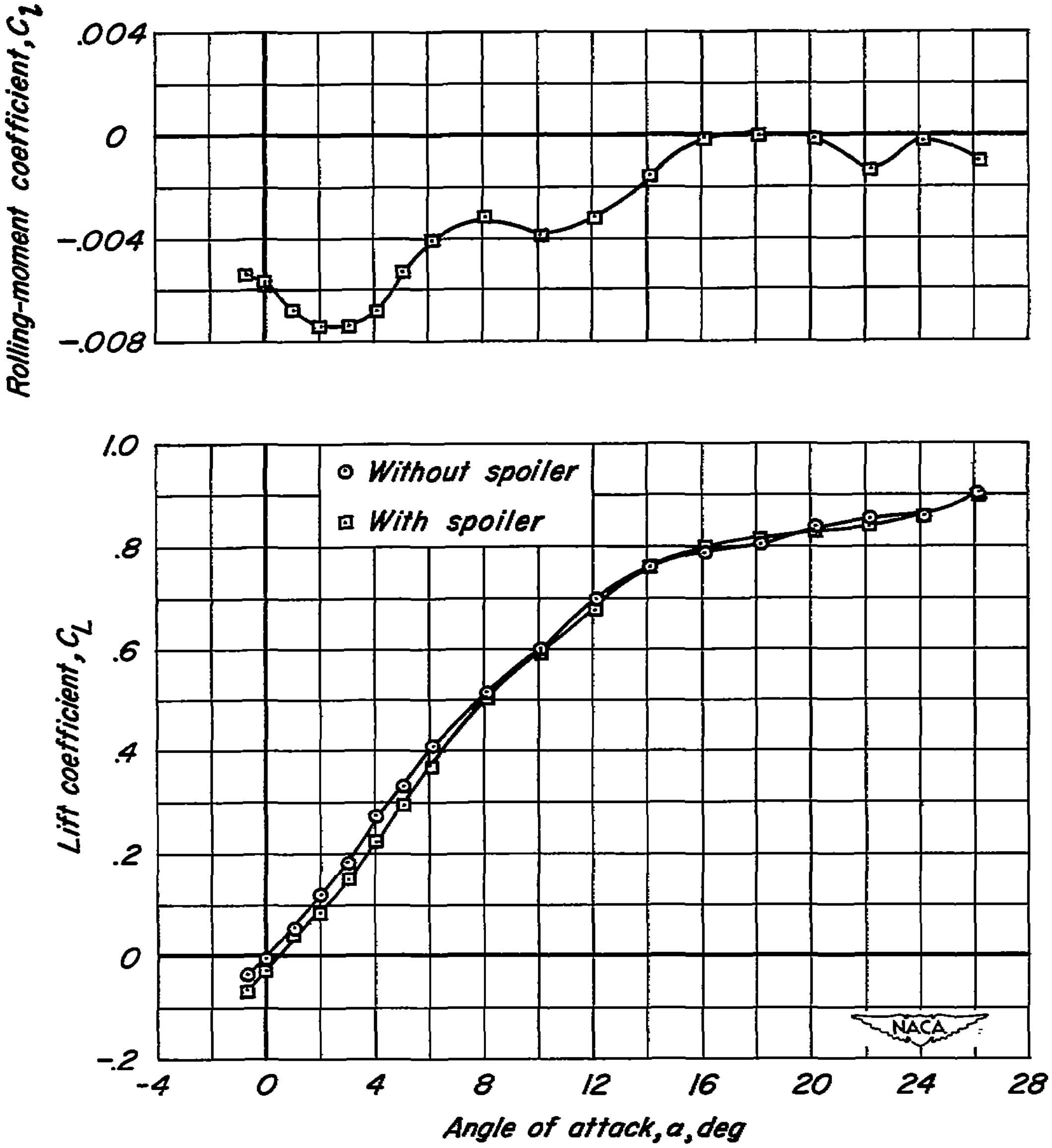

(a) C_l vs α, C_L vs α

Figure 4.—The aerodynamic characteristics at a Mach number of 0.60. R=1,500,000.

[redacted]

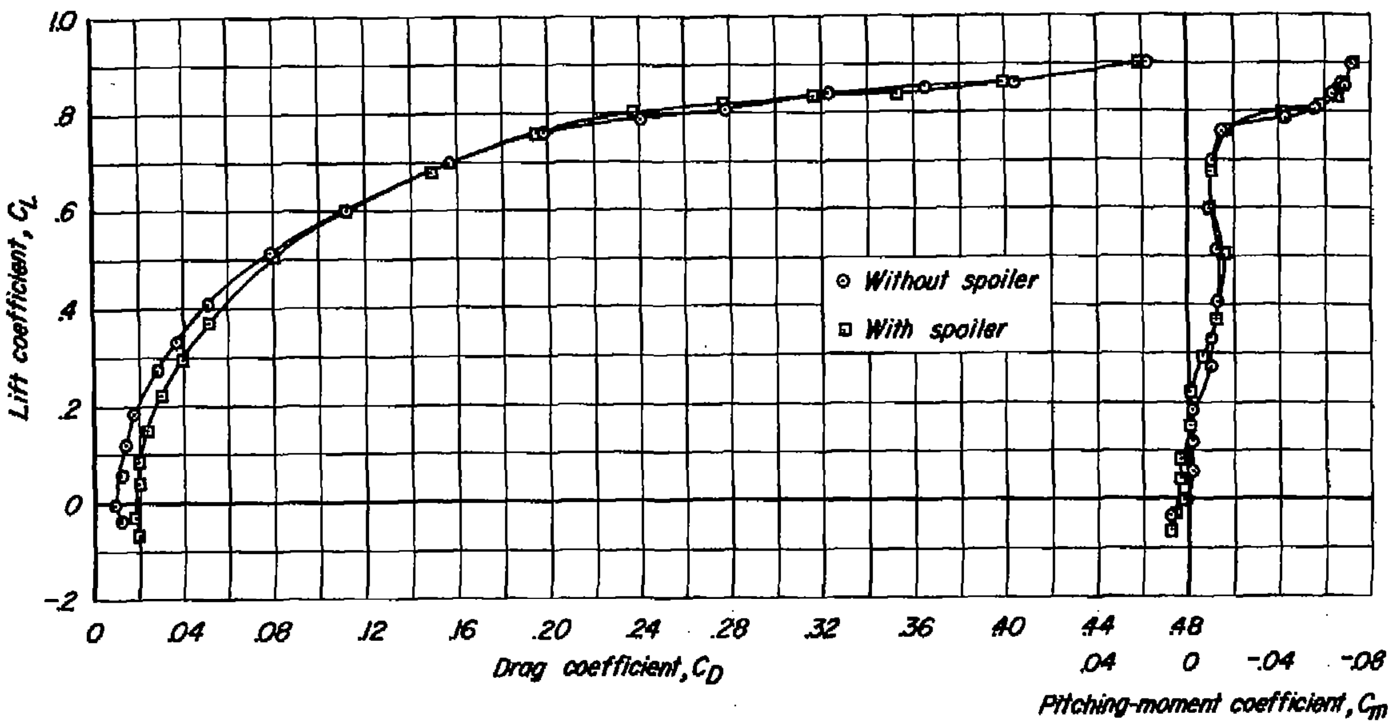

(b) C_L vs C_D, C_L vs C_m

Figure 4.-Concluded.

[redacted]

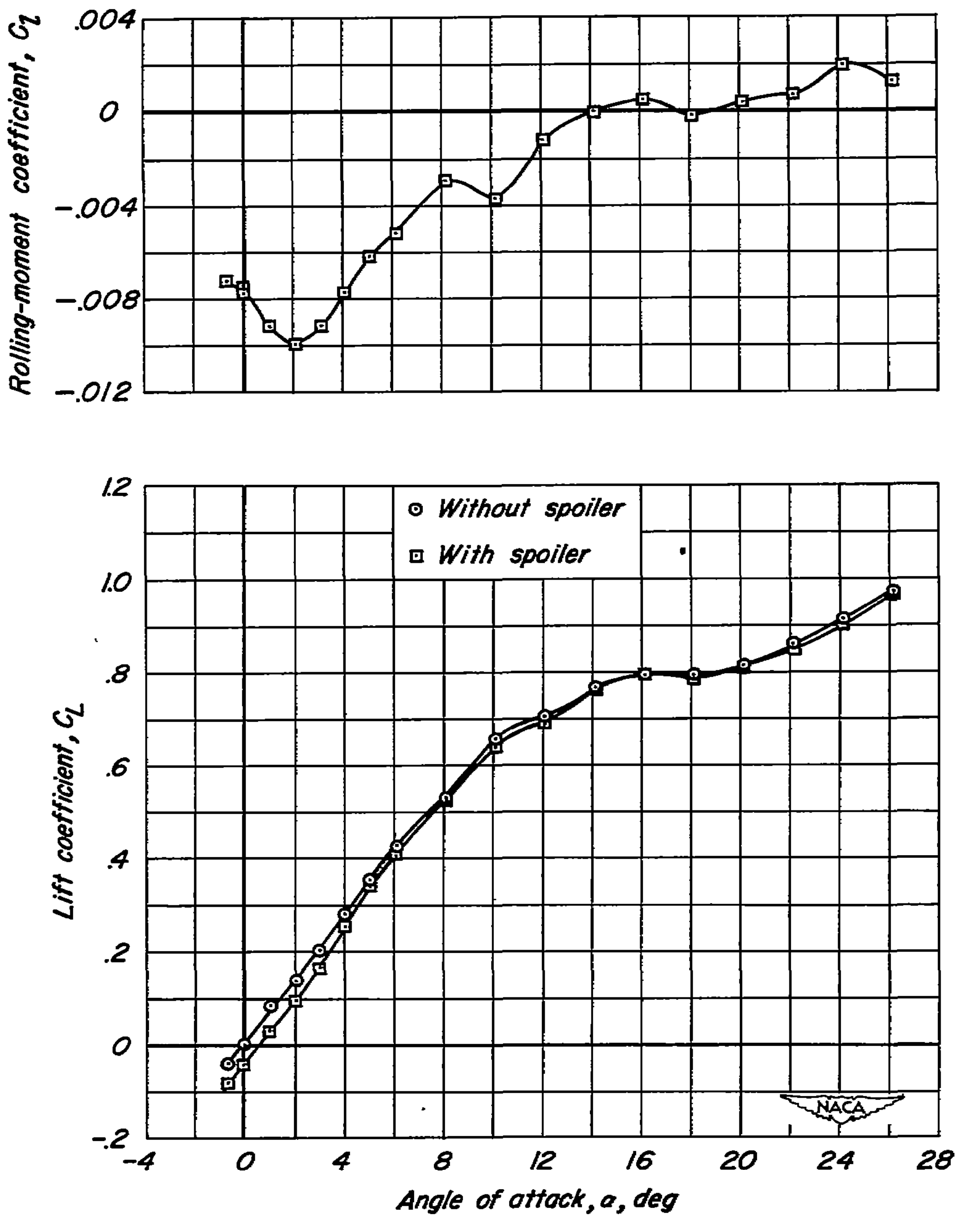

(a) C_l vs α , C_L vs α

Figure 5.– The aerodynamic characteristics at a Mach number of 0.80. R = 1,500,000.

[redacted]

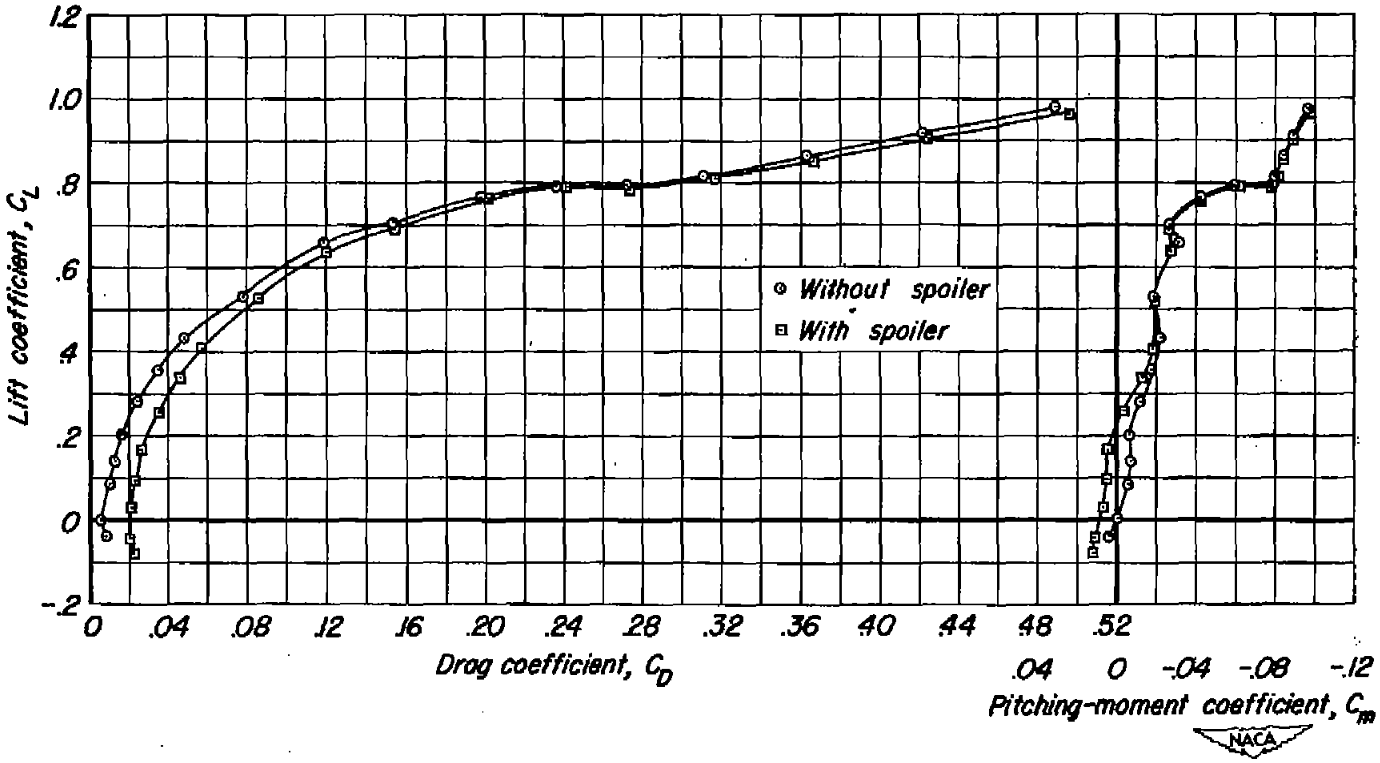

[redacted]

(b) C_L vs C_D, C_L vs C_m

Figure 5.—Concluded.

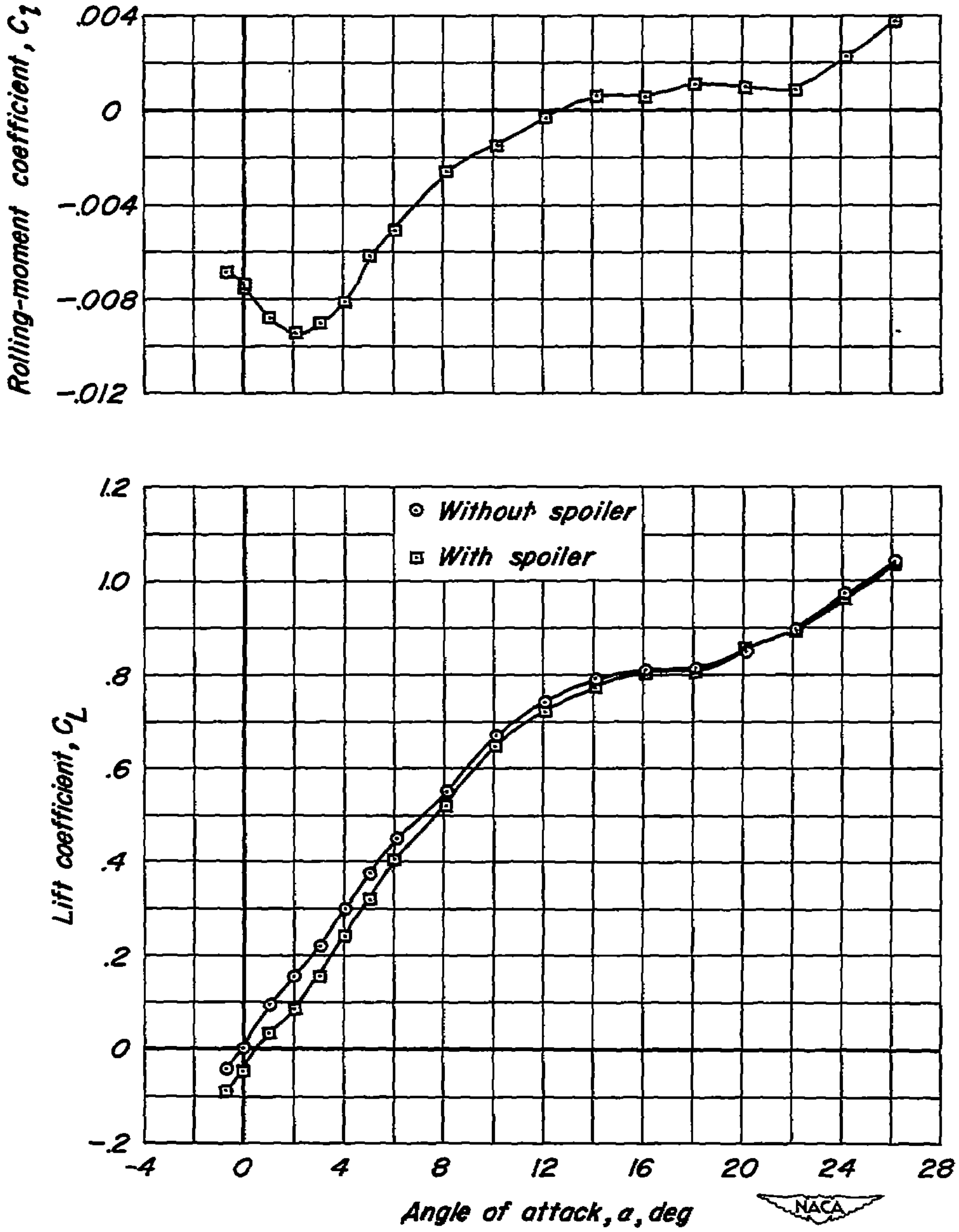

(a) C_l vs α, C_L vs α

Figure 6.—The aerodynamic characteristics at a Mach number of 0.85. R = 1,500,000.

[redacted]

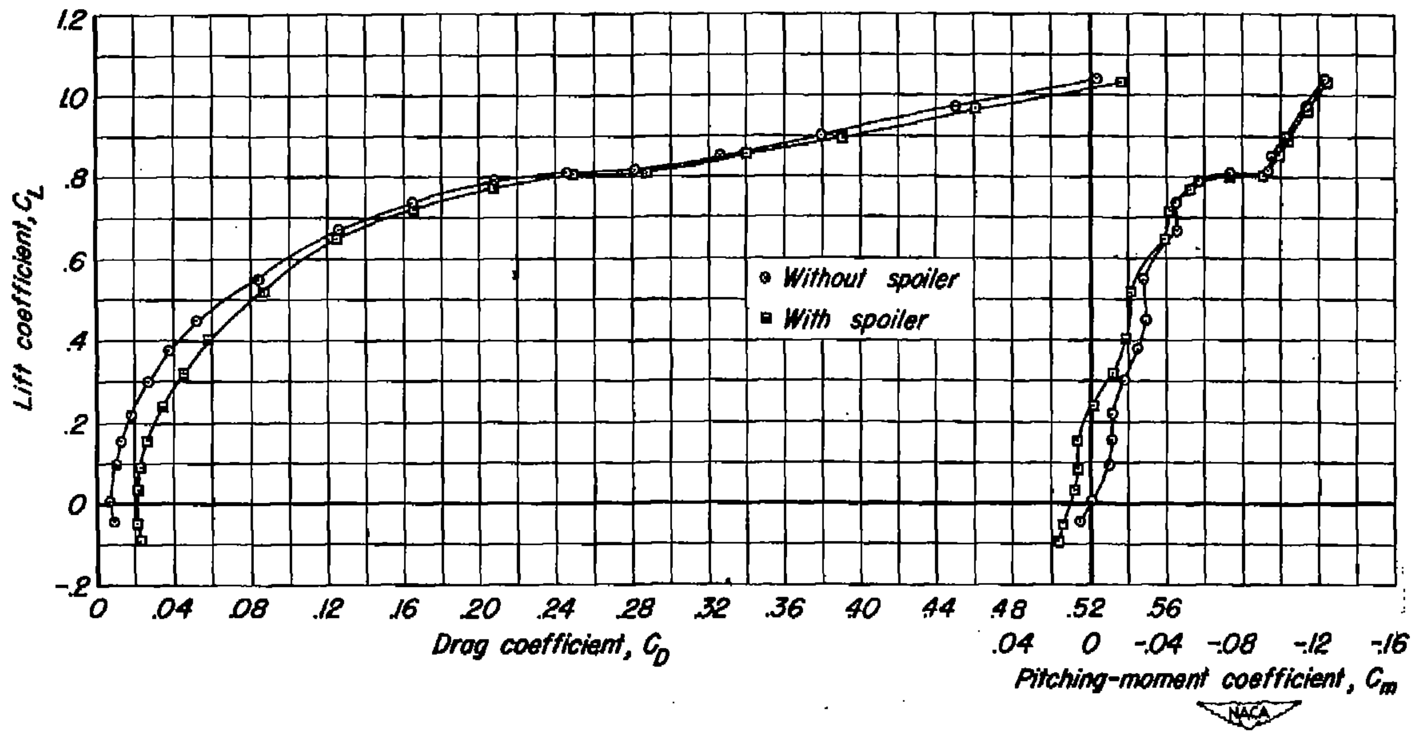

(b) C_L vs C_D, C_L vs C_m

Figure 6.–Concluded.

[redacted]

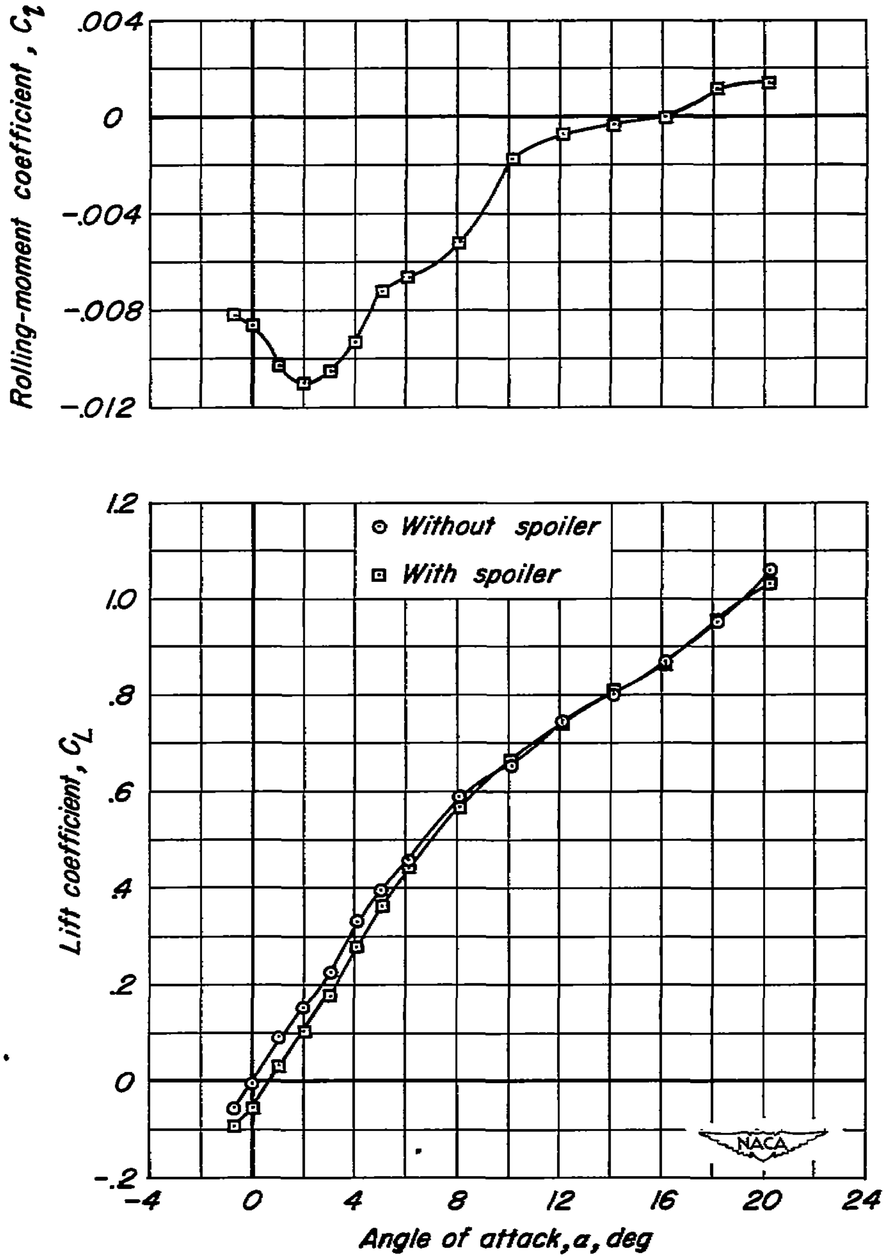

(a) C_l vs α, C_L vs α

Figure 7.- The aerodynamic characteristics at a Mach number of 0.90. R=1,500,000.

[redacted]

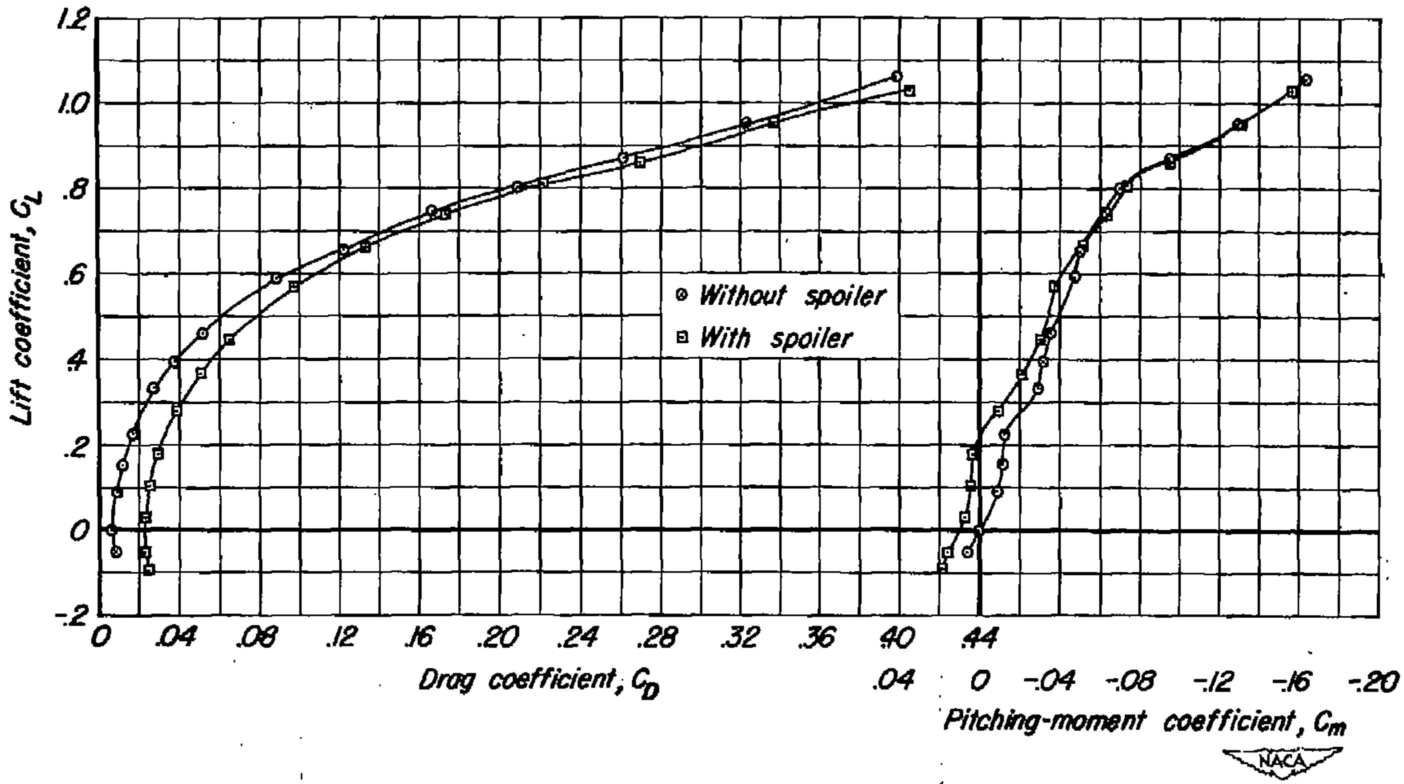

(b) C_L vs C_D, C_L vs C_m

Figure 7.-Concluded.

[redacted]

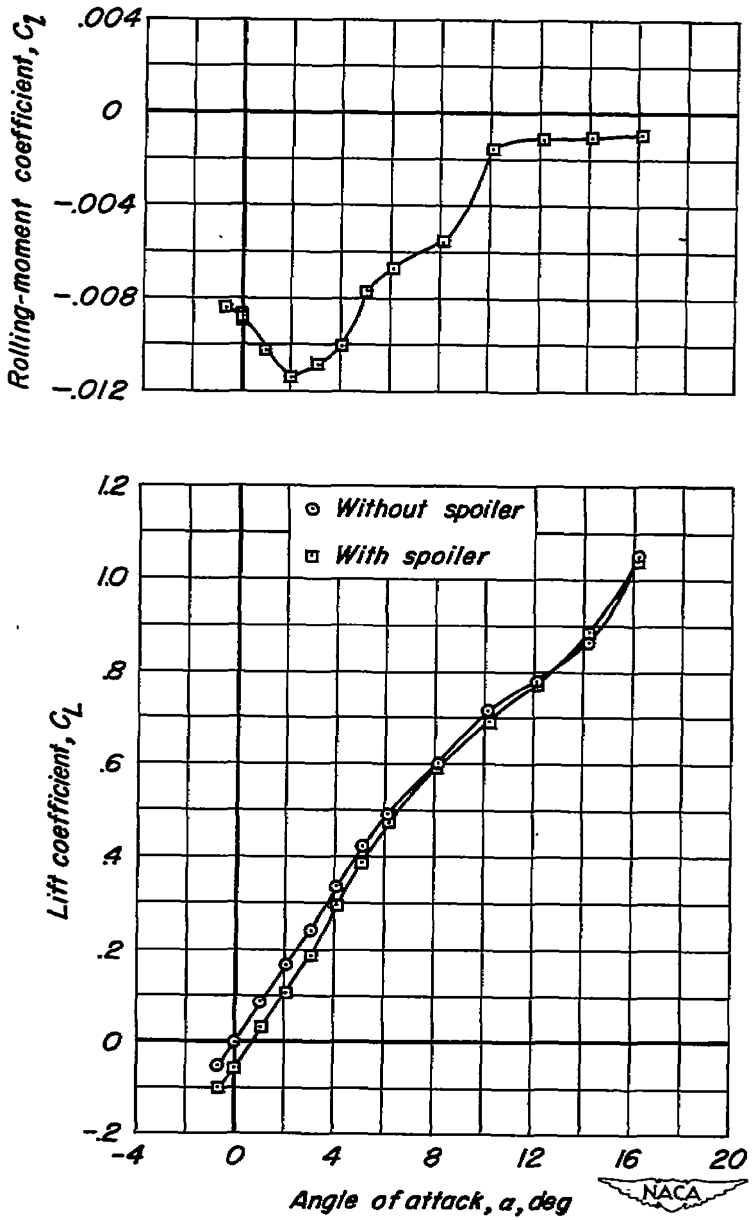

(a) C_l vs α, C_L vs α

Figure 8.–The aerodynamic characteristics at a Mach number of 0.92. R=1,500,000.

[redacted]

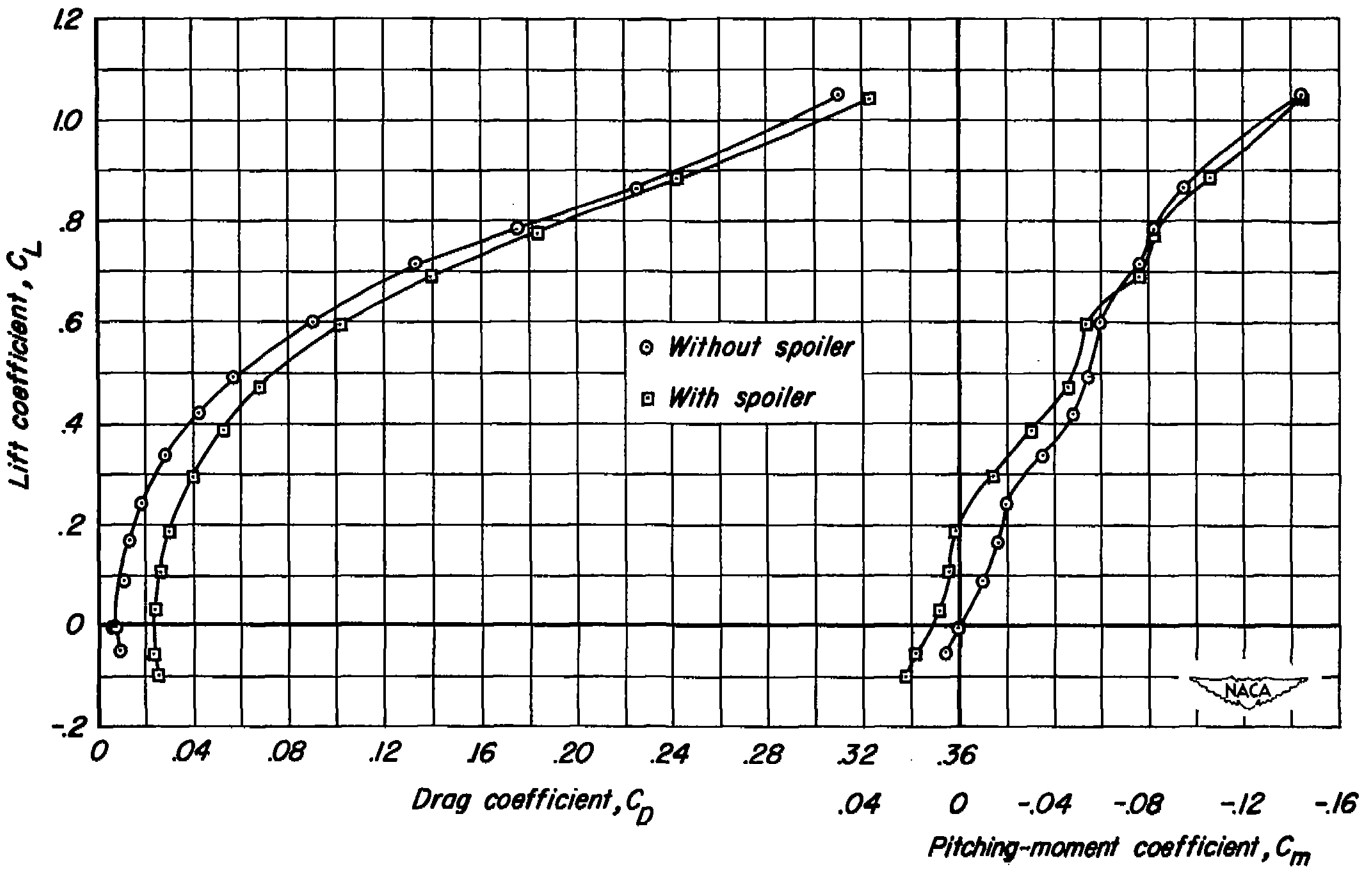

(b) C_L vs C_D, C_L vs C_m

Figure 8.– Concluded.

[redacted]

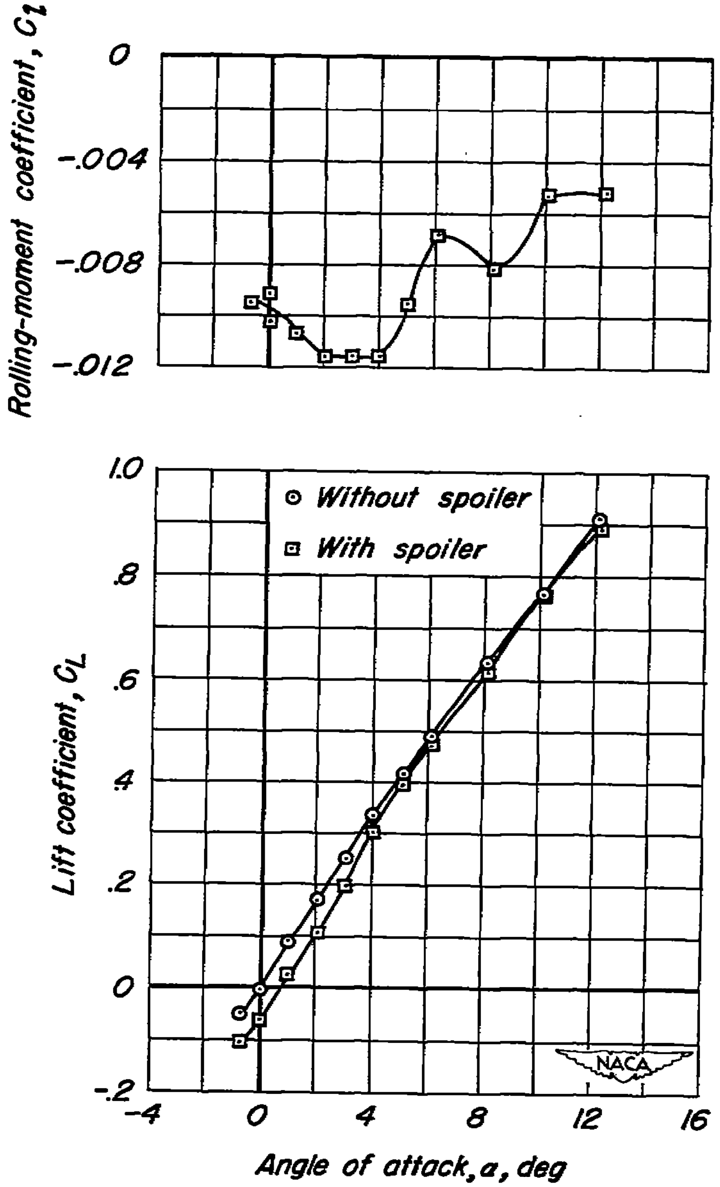

(a) C_l vs α, C_L vs α

Figure 9.–The aerodynamic characteristics at a Mach number of 0.94. R=1,500,000.

[redacted]

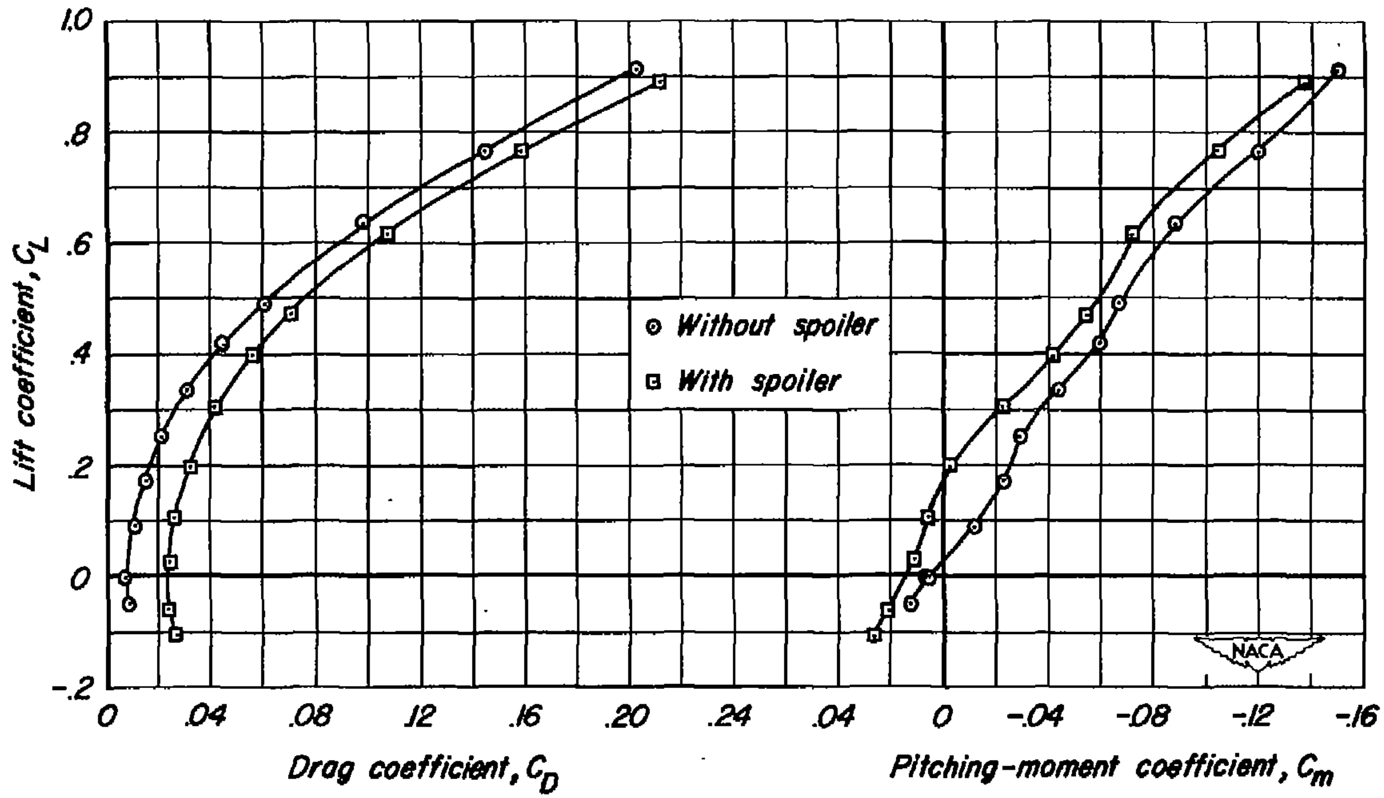

(b) C_L vs C_D, C_L vs C_m

Figure 9.—Concluded.

[redacted]

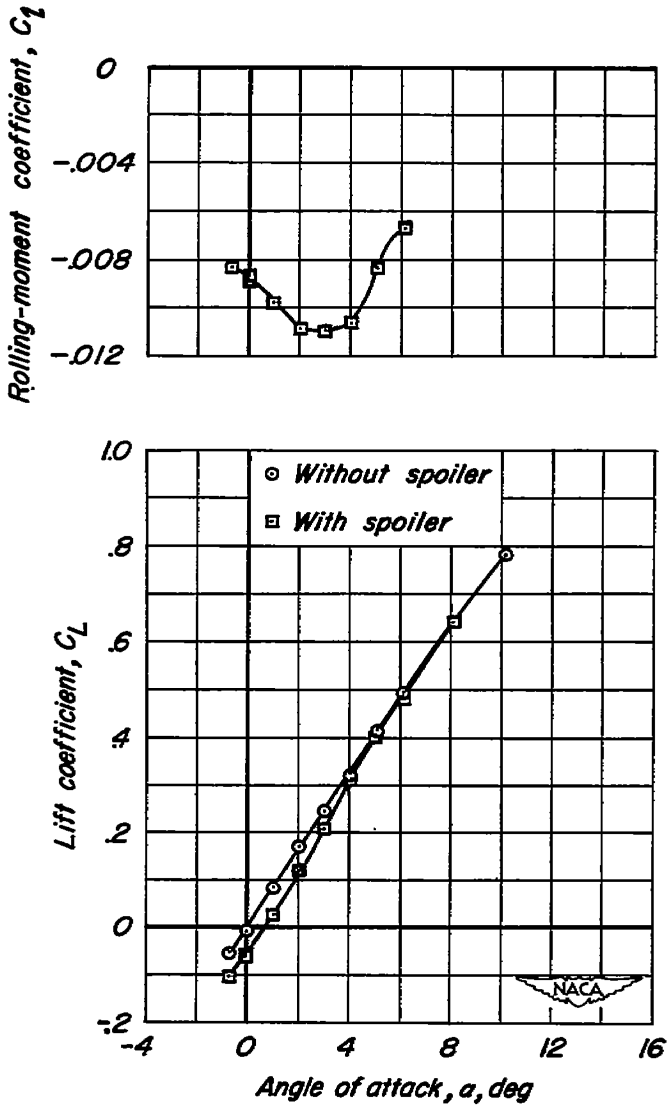

(a) C_l vs α, C_L vs α

Figure 10.– The aerodynamic characteristics at a Mach number of 0.96. R = 1,500,000.

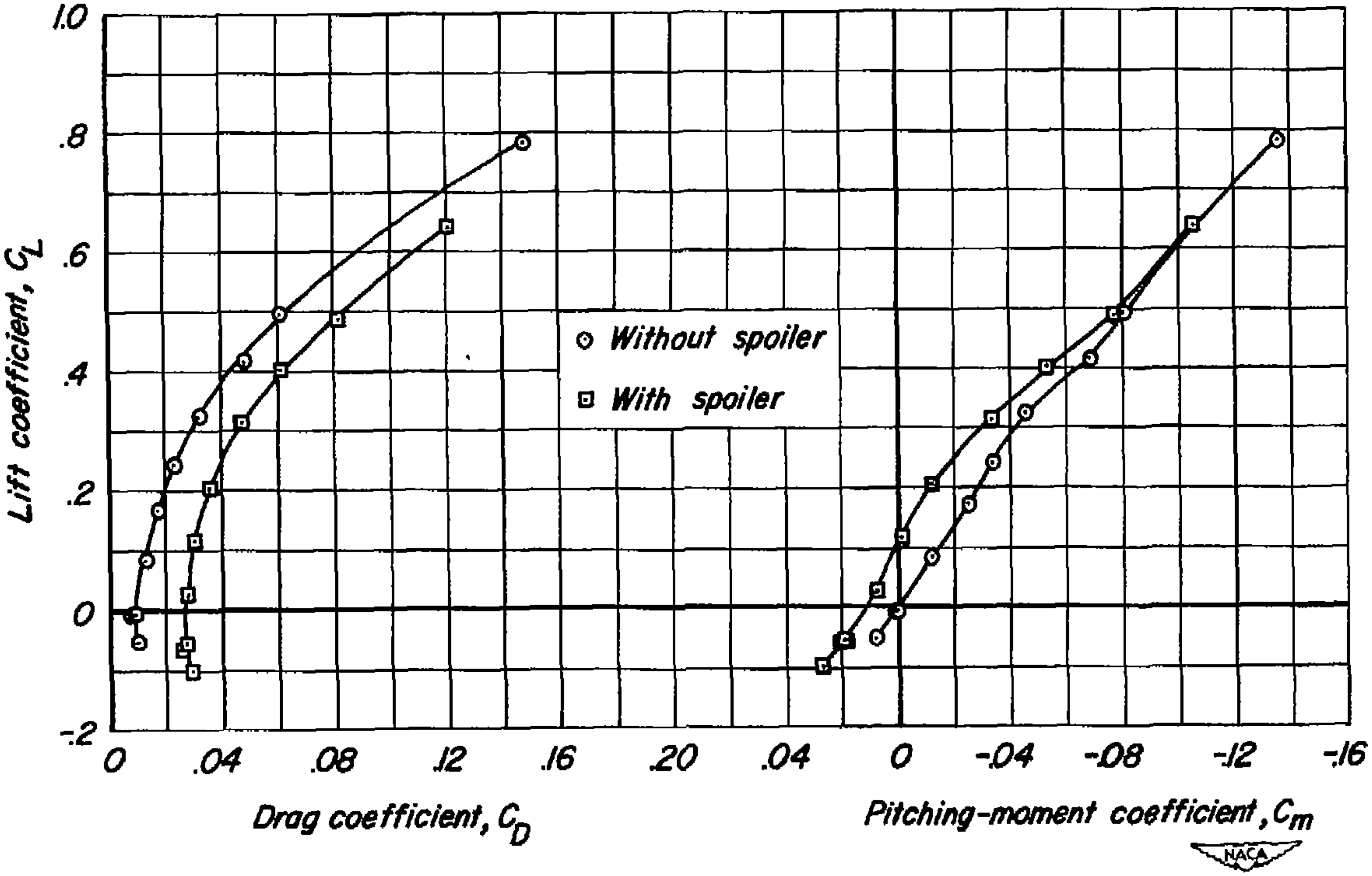

(b) C_L vs C_D, C_L vs C_m

Figure 10.—Concluded.

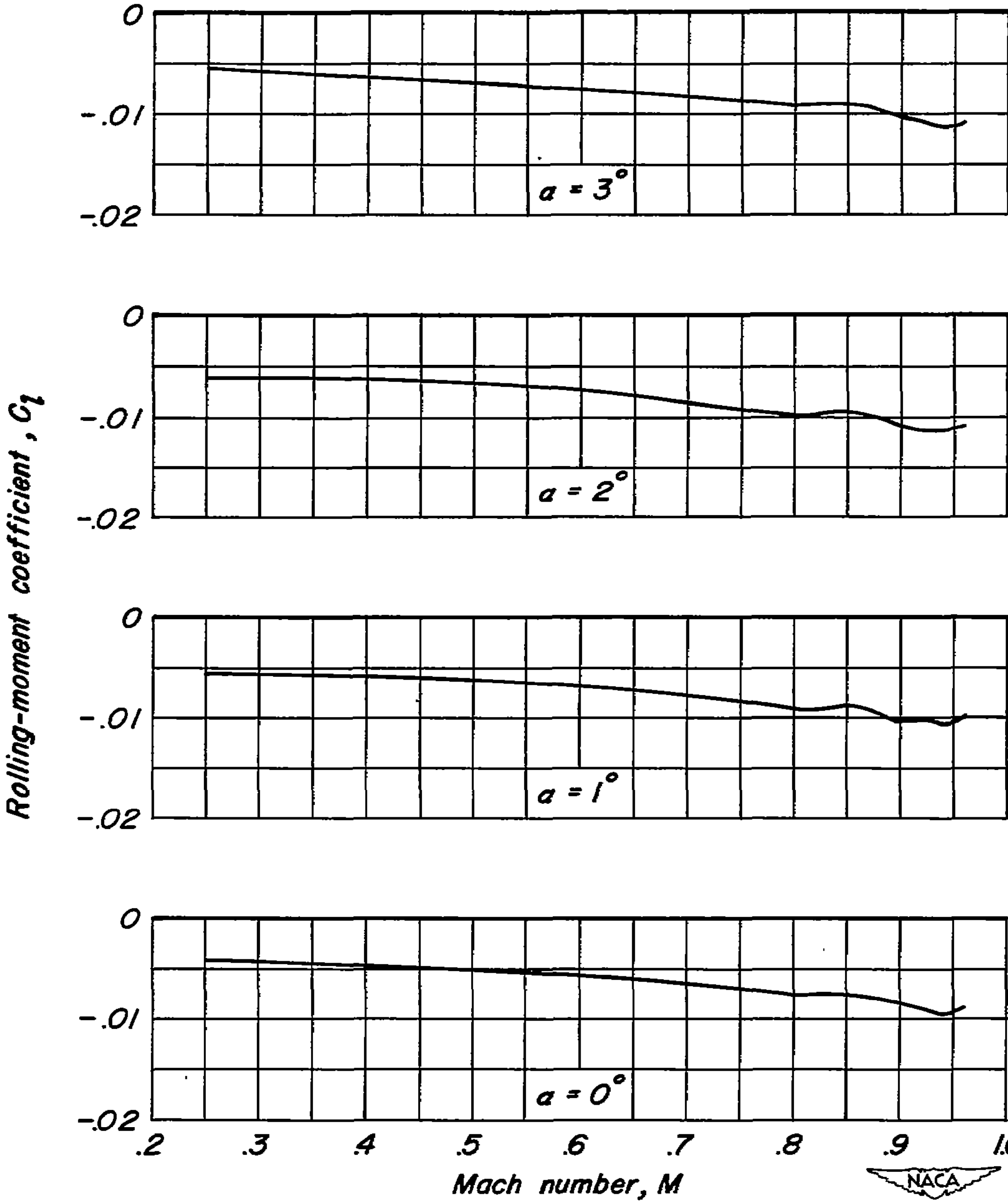

(a) $\alpha = 0^\circ, 1^\circ, 2^\circ, 3^\circ$

Figure 11.– Variation with Mach number of rolling-moment coefficient for a model with a perforated spoiler. R = 1,500,000.

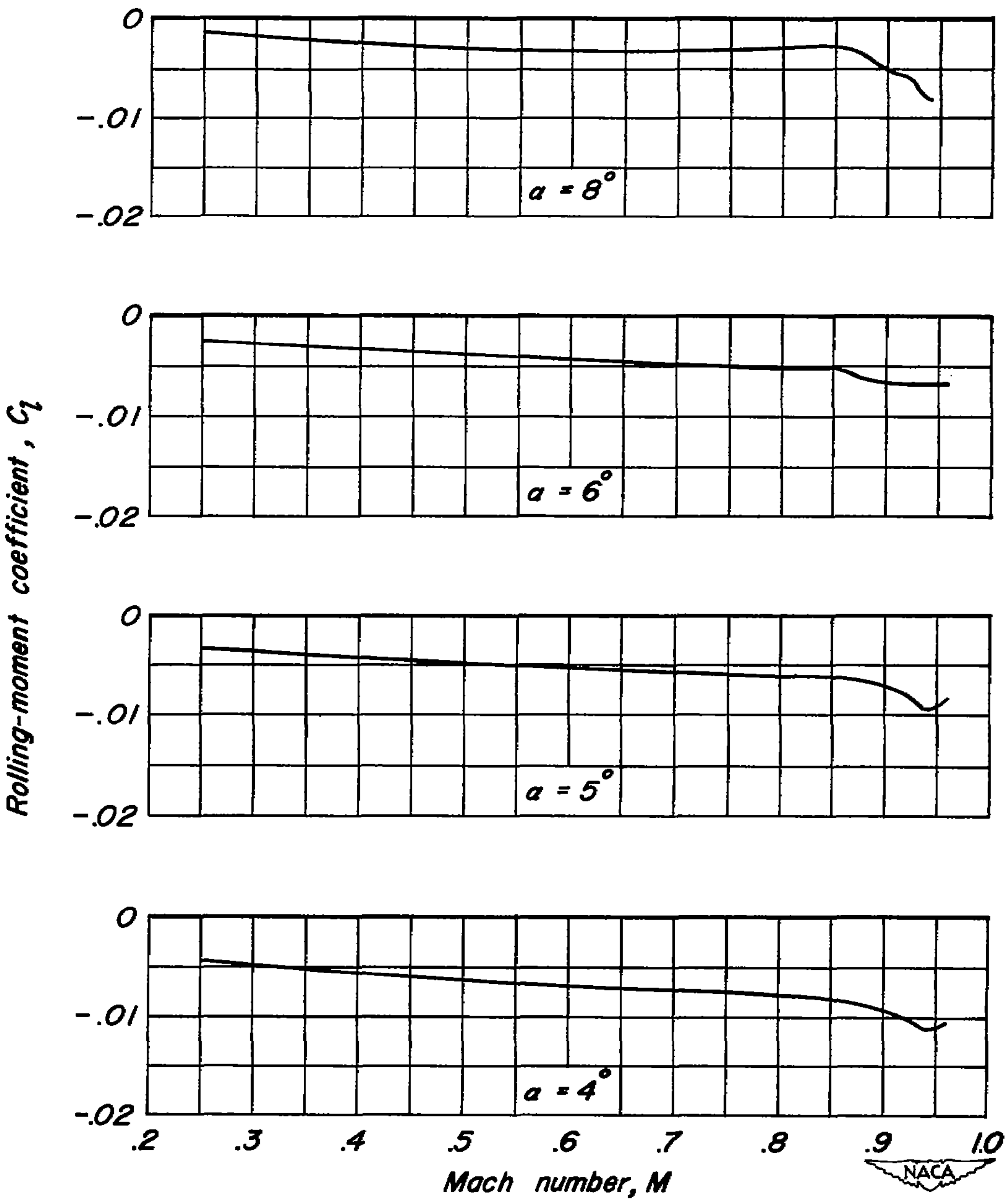

(b) α=4°, 5°, 6°, 8°

Figure 11.- Concluded.

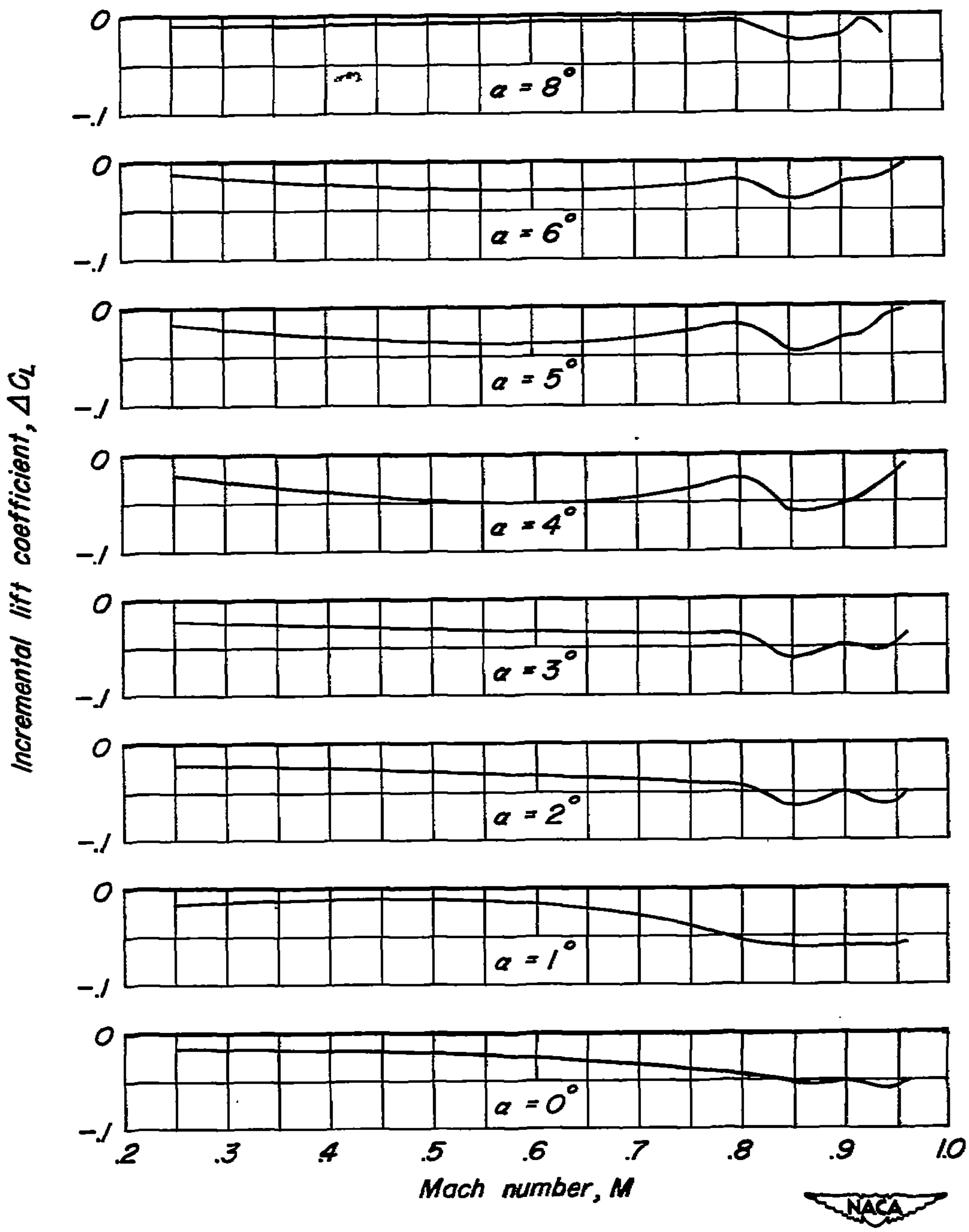

Figure 12.–Variation with Mach number of incremental lift coefficient for a model with a perforated spoiler. R = 1,500,000.

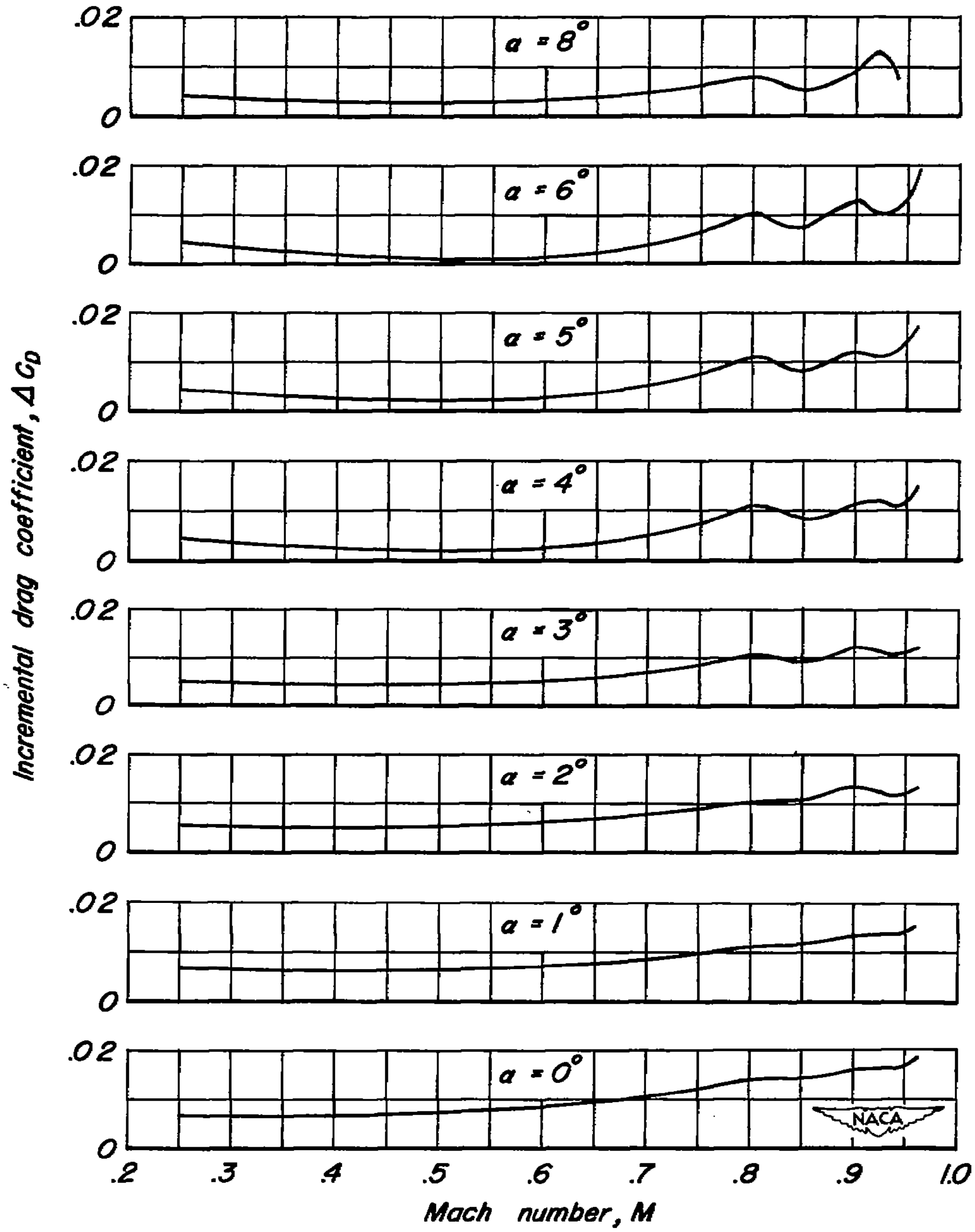

Figure 13.- Variation with Mach number of incremental drag coefficient for a model with a perforated spoiler. R = 1,500,000.

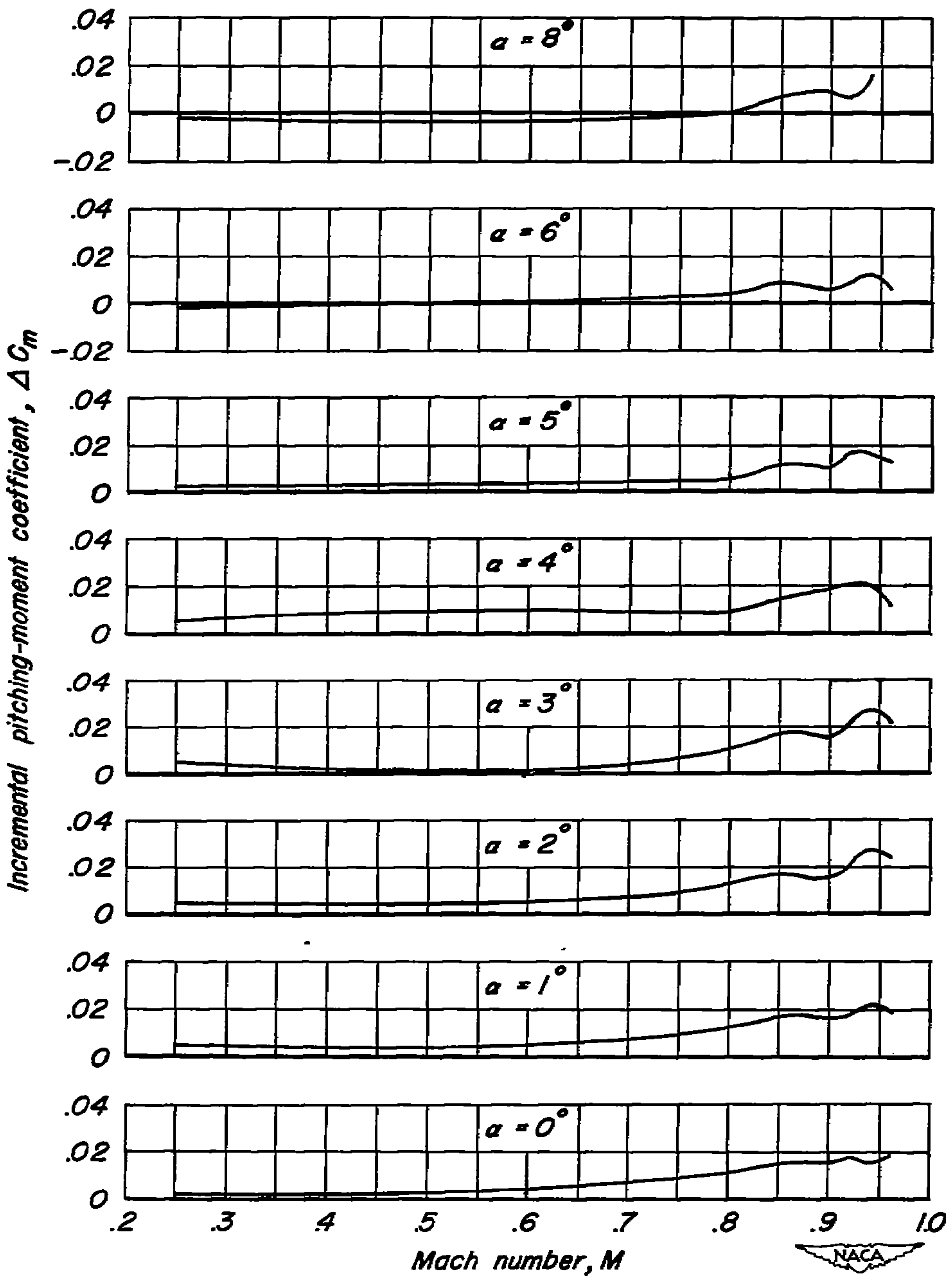

Figure 14.—Variation with Mach number of incremental pitching-moment coefficient for a model with a perforated spoiler. R = 1,500,000.

[redacted]

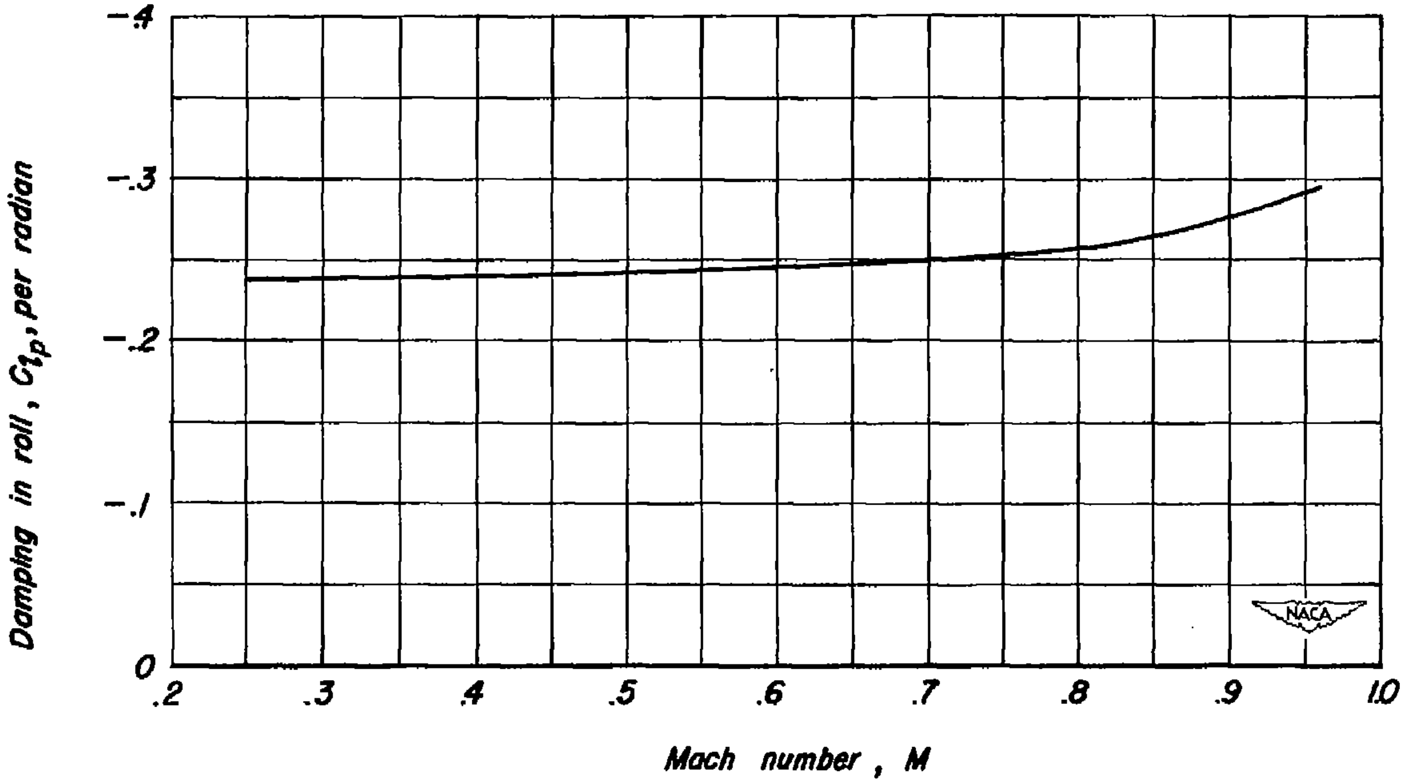

Figure 15.– Variation with Mach number of the calculated damping in roll for a wing of aspect ratio 3 and having 45° of sweepback. $\alpha = 0°$.

[redacted]

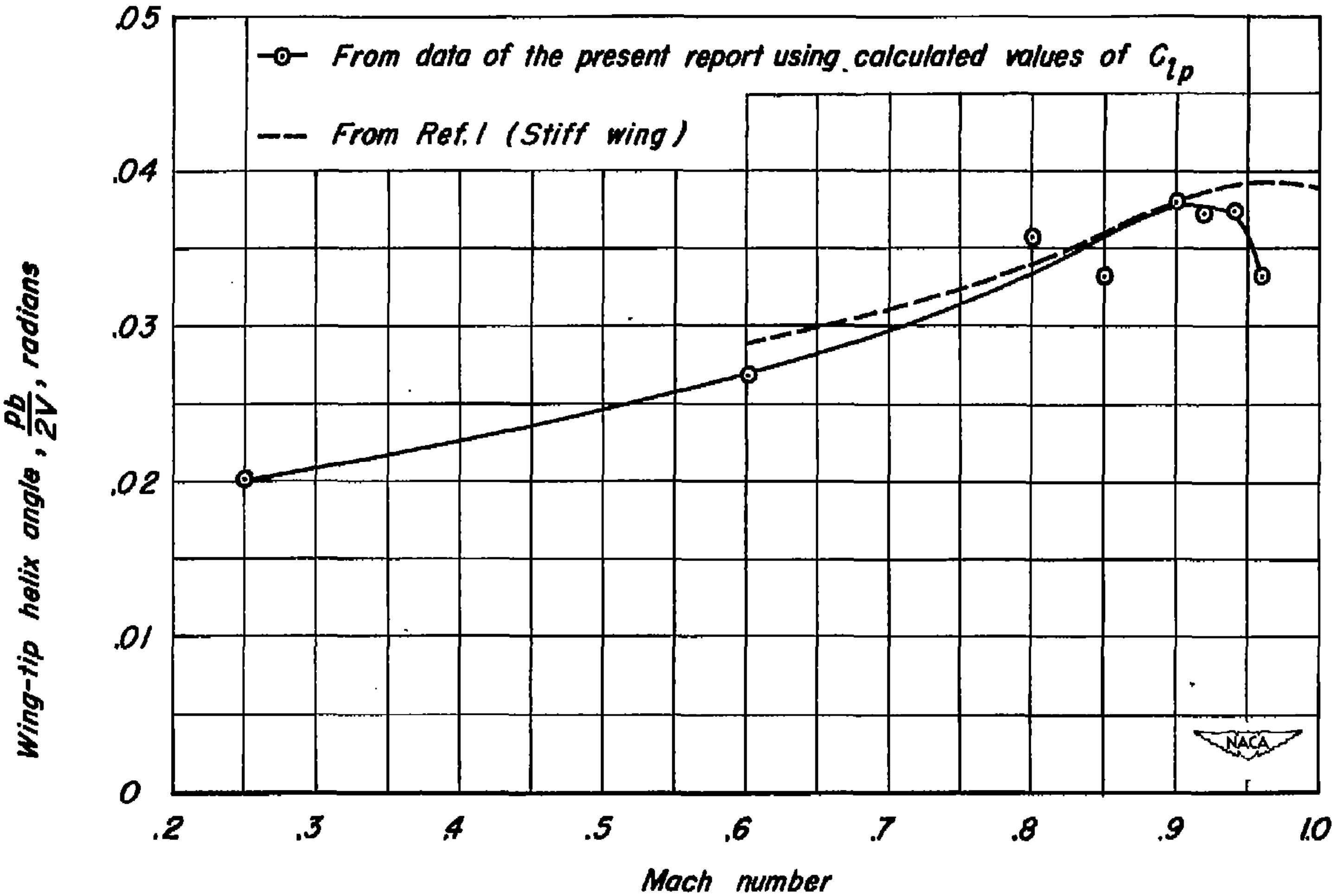

Figure 16.– Variation with Mach number of wing-tip helix angle due to projection of the perforated spoiler. $\alpha = 0°$, $R = 1{,}500{,}000$.

[redacted]

[redacted]